

## Supplementary information

### *Self-assembly Processes of Octahedron-shaped Pd<sub>6</sub>L<sub>12</sub> Cages*

Shohei Komine, Tomoki Tateishi, Tatsuo Kojima, Haruna Nakagawa, Yasuhiro Hayashi, Satoshi Takahashi, and Shuichi Hiraoka\*

*Department of Basic Science, Graduate School of Arts and Sciences*

*The University of Tokyo*

*3-8-1 Komaba, Meguro-ku, Tokyo 153-8902, Japan*

*E-mail: chiraoka@mail.ecc.u-tokyo.ac.jp*

## Contents

• General Information	···S2
• Materials	···S2
• Quantitative analysis of self-assembly process for [Pd <sub>6</sub> L <sub>12</sub> ](BF <sub>4</sub> ) <sub>12</sub> cages	···S2
• Monitoring of the self-assembly of [Pd <sub>6</sub> L <sub>12</sub> ](BF <sub>4</sub> ) <sub>12</sub> complexes by <sup>1</sup> H NMR	
· Procedure for monitoring the self-assembly process of [Pd <sub>6</sub> L <sub>12</sub> ](BF <sub>4</sub> ) <sub>12</sub> complexes	···S3
· Determination of the existence ratios of each species	···S4
· <sup>1</sup> H NMR spectra for the self-assembly of [Pd <sub>6</sub> L <sub>12</sub> ](BF <sub>4</sub> ) <sub>12</sub> complexes	
· [Pd <sub>6</sub> <b>1</b> <sup>S</sup> <sub>12</sub> ](BF <sub>4</sub> ) <sub>12</sub> in CD <sub>3</sub> NO <sub>2</sub> (Figure S1)	···S6
· [Pd <sub>6</sub> <b>2</b> <sub>12</sub> ](BF <sub>4</sub> ) <sub>12</sub> in CD <sub>3</sub> NO <sub>2</sub> and CD <sub>2</sub> Cl <sub>2</sub> (4:1, v/v) (Figure S2)	···S7
· [Pd <sub>6</sub> <b>3</b> <sub>12</sub> ](BF <sub>4</sub> ) <sub>12</sub> in CD <sub>3</sub> NO <sub>2</sub> and CD <sub>2</sub> Cl <sub>2</sub> (4:1, v/v) (Figure S3)	···S8
· Time variation of L, [PdPy* <sub>4</sub> ](BF <sub>4</sub> ) <sub>2</sub> , [Pd <sub>6</sub> L <sub>12</sub> ](BF <sub>4</sub> ) <sub>12</sub> , Py*, <b>Int</b> , and the ( <i>&lt;n&gt;</i> , <i>&lt;k&gt;</i> ) values for the self-assembly of [Pd <sub>6</sub> L <sub>12</sub> ](BF <sub>4</sub> ) <sub>12</sub> complexes	
· [Pd <sub>6</sub> <b>1</b> <sup>S</sup> <sub>12</sub> ](BF <sub>4</sub> ) <sub>12</sub> in CD <sub>3</sub> NO <sub>2</sub> (Tables S1–S5)	···S9
· [Pd <sub>6</sub> <b>2</b> <sub>12</sub> ](BF <sub>4</sub> ) <sub>12</sub> in CD <sub>3</sub> NO <sub>2</sub> and CD <sub>2</sub> Cl <sub>2</sub> (4:1, v/v) (Tables S6–S10)	···S14
· [Pd <sub>6</sub> <b>3</b> <sub>12</sub> ](BF <sub>4</sub> ) <sub>12</sub> in CD <sub>3</sub> NO <sub>2</sub> and CD <sub>2</sub> Cl <sub>2</sub> (4:1, v/v) (Tables S11–S15)	···S19
• Monitoring of the self-assembly of [Pd <sub>6</sub> L <sub>12</sub> ](BF <sub>4</sub> ) <sub>12</sub> complexes by ESI-TOF mass spectrometry	
· [Pd <sub>6</sub> <b>1</b> <sup>S</sup> <sub>12</sub> ](BF <sub>4</sub> ) <sub>12</sub> in CD <sub>3</sub> NO <sub>2</sub> (Figure S4)	···S24
· [Pd <sub>6</sub> <b>2</b> <sub>12</sub> ](BF <sub>4</sub> ) <sub>12</sub> in CD <sub>3</sub> NO <sub>2</sub> and CD <sub>2</sub> Cl <sub>2</sub> (4:1, v/v) (Figure S5)	···S30
· [Pd <sub>6</sub> <b>3</b> <sub>12</sub> ](BF <sub>4</sub> ) <sub>12</sub> in CD <sub>3</sub> NO <sub>2</sub> and CD <sub>2</sub> Cl <sub>2</sub> (4:1, v/v) (Figure S6)	···S32
• Molecular modeling study	
· Optimized structures of double-walled motifs <i>cis</i> -[Pd <sub>2</sub> L <sub>2</sub> Py <sub>4</sub> ] <sup>4+</sup> (Py: pyridine) for ditopic ligands <b>2</b> and <b>3</b> (Figure S7)	···S36
• References	···S36

## General Information

<sup>1</sup>H NMR spectra were recorded using a Bruker AV-500 (500 MHz) spectrometer. All <sup>1</sup>H NMR spectra were referenced using a residual solvent peak, CD<sub>3</sub>NO<sub>2</sub> ( $\delta$  4.33). Electrospray ionization time-of-flight (ESI-TOF) mass spectra were obtained using a Waters Xevo G2-S Tof mass spectrometer. Dynamic light scattering (DLS) measurements were performed using a Malvern Zetasizer Nano ZS instrument equipped with a He-Nelaser operating at 2 mW power and 633 nm wavelength, and a computer-controlled correlator, at 173° accumulation angle. Tapping mode AFM (Atomic Force Microscopy) experiments were executed with a NanoNavi S-image instrument (SII, Tokyo, Japan).

## Materials

Unless otherwise noted, all solvents and reagents were obtained from commercial suppliers (TCI Co., Ltd., WAKO Pure Chemical Industries Ltd., KANTO Chemical Co., Inc., and Sigma-Aldrich Co.) and were used as received. CD<sub>3</sub>NO<sub>2</sub> was purchased from Acros Organics and used after dehydration with Molecular Sieves 4Å. Ditopic ligand **1**,<sup>1</sup> **2**,<sup>2</sup> and **3**<sup>3</sup> and [PdPy\*<sub>4</sub>](BF<sub>4</sub>)<sub>2</sub><sup>4</sup> were prepared according to the literature.

### Quantitative analysis of self-assembly process for [Pd<sub>6</sub>L<sub>12</sub>](BF<sub>4</sub>)<sub>12</sub> cages

The self-assembly processes of the [Pd<sub>6</sub>L<sub>12</sub>]<sup>12+</sup> cages were investigated by QASAP (quantitative analysis of self-assembly process). In many coordination self-assemblies, the signals for most of the intermediates transiently produced during the self-assembly cannot be observed by NMR spectroscopy, which prevents us from directly obtaining the information about the intermediates. In QASAP, the average composition of all the intermediates can be obtained by the quantification of all the substrates and products. Thus, QASAP allows us to discuss the self-assembly processes from the time-development of the average composition of all the intermediates even if none of the intermediates cannot be detected. The self-assembly of [Pd<sub>6</sub>L<sub>12</sub>]<sup>12+</sup> cages from Pd(II) ions and ditopic ligands, L, is expressed by the following equation.



where X is a leaving ligand that originally binds to the Pd(II) ions of the metal source. 3-Chloropyridine (Py\*) was used as X in this research. All the intermediates in the self-assembly of the cages are expressed by [Pd<sub>a</sub>L<sub>b</sub>X<sub>c</sub>]<sup>2a+</sup> (*a*–*c* are the number of each component). What is obtained by QASAP is the average composition of all the intermediates, [Pd<sub>*a*</sub>L<sub>*b*</sub>X<sub>*c*</sub>]<sup>2*a*+</sup>. In order to investigate the self-assembly processes from the time-development of [Pd<sub>*a*</sub>L<sub>*b*</sub>X<sub>*c*</sub>]<sup>2*a*+</sup>, the following two parameters are introduced.

$$\langle n \rangle = \frac{4\langle a \rangle - \langle c \rangle}{\langle b \rangle} \quad (2)$$

$$\langle k \rangle = \frac{\langle a \rangle}{\langle b \rangle} \quad (3)$$

The  $\langle n \rangle$  value indicates the average number of Pd(II) ions that bind to a single ditopic ligand L, so the maximum of the  $\langle n \rangle$  value is 2. The  $\langle k \rangle$  value indicates the stoichiometric ratio between Pd(II) ions and the ditopic ligands L in [Pd<sub>*a*</sub>L<sub>*b*</sub>X<sub>*c*</sub>]<sup>2*a*+</sup>. The change in the ( $\langle n \rangle$ ,  $\langle k \rangle$ ) value enables us to deduce not only predominant intermediates but also reaction types (incorporation of components in

intermediates, growth of intermediates, and production of final assembly from intermediates) in the self-assembly process.

## Monitoring of the self-assembly of $[Pd_6L_{12}](BF_4)_{12}$ complexes by $^1H$ NMR

### Procedure for monitoring the self-assembly process of $[Pd_6L_{12}](BF_4)_{12}$ complexes

A 2.4 mM solution of [2.2]paracyclophe in  $CHCl_3$  (125  $\mu L$ ), which was used as an internal standard, was added to two NMR tubes (tubes **I** and **II**) and the solvent was removed in vacuo. A solution of  $[PdPy^*_4](BF_4)_2$  (12 mM) in  $CD_3NO_2$  was prepared (solution **A**). Solution **A** (50  $\mu L$ ) and  $CD_3NO_2$  (450  $\mu L$ ) were added to tube **I**. The exact concentration of  $[PdPy^*_4](BF_4)_2$  in solution **A** was determined through the comparison of the signal intensity with [2.2]paracyclophe by  $^1H$  NMR. A solution of ditopic ligand, L (**1<sup>S</sup>**, **2**, or **3**), (12 mM) in  $CHCl_3$  (100  $\mu L$ ) was added to tube **II** and the solvent was removed in vacuo. Then  $CD_3NO_2$  (550  $\mu L$ ) for **1<sup>S</sup>** or a mixed solvent of  $CD_2Cl_2$  (120  $\mu L$ ) and  $CD_3NO_2$  (430  $\mu L$ ) for **2** and **3** was added to tube **II** and the exact amount of L in tube **II** was determined through the comparison of the signal intensity with [2.2]paracyclophe by  $^1H$  NMR. 0.50 eq. (against the amount of ligand L in tube **II**) of solution **A** (*ca.* 50  $\mu L$ ; the exact amount was determined based on the exact concentration of solution **A** and of ligand in tube **II**) were added to tube **II** at 263 K. The self-assembly of the  $[Pd_6L_{12}](BF_4)_{12}$  was monitored at 298 K by  $^1H$  NMR spectroscopy. Examples of the  $^1H$  NMR spectra are shown in Figures 2, 5, 8, S1, S2, and S3. The exact ratio of L and  $[PdPy^*_4](BF_4)_2$  was unambiguously determined by the comparison of the integral value of each  $^1H$  signal of [2.2]paracyclophe. The amounts of L,  $[PdPy^*_4](BF_4)_2$ ,  $[Pd_6L_{12}](BF_4)_{12}$ , and Py\* were quantified by the integral value of each  $^1H$  signal against the signal of the internal standard ([2.2]paracyclophe). In order to confirm the reproducibility, the same experiment was carried out three times (runs 1–3 for **1<sup>S</sup>**, 4–6 for **2**, and 7–9 for **3**) in total. These data, the average values of the existence ratios and the ( $\langle n \rangle$ ,  $\langle k \rangle$ ) values are listed in Tables S1–S5 for **1<sup>S</sup>**, S6–S10 for **2**, and S11–S15 for **3**. Standard errors shown in Figure S2, S7 and S12 were calculated based on the three runs.

Authentic samples of the final assemblies,  $Pd_6L_{12}$  (L = **1–3**), were obtained according to the original papers of the cages. Then the solvent was replaced with  $CD_3NO_2$  and  $CD_2Cl_2$  (4:1, v/v) or  $CD_3NO_2$  before the  $^1H$  NMR measurement.



species containing L (free L and  $[Pd_6L_{12}]^{12+}$ ) from the total amount of L ( $I_L(0)$ ). The existence ratio of **Int** at  $t$  is expressed by  $(I_L(0) - I_L(t) - I_{cage}(t))/I_L(0)$ .

$\langle a \rangle$

The total amount of Pd(II) ions corresponds to  $I_M(0)/4$ . The amount of Pd(II) ions in  $[PdPy^*_4]^{2+}$  at  $t$  corresponds to  $I_M(t)/4$ . The amount of Pd(II) ions in  $[Pd_6L_{12}]^{12+}$  at  $t$  corresponds to  $I_{cage}(t)/2$ , respectively. The amount of Pd(II) ions in **Int** at  $t$  is thus expressed by  $I_M(0)/4 - I_M(t)/4 - I_{cage}(t)/2$ .

$\langle b \rangle$

The total amount of ligand L corresponds to  $I_L(0)$ . The amount of free ligand L at  $t$  corresponds to  $I_L(t)$ . The amounts of ligand L in  $[Pd_6L_{12}]^{12+}$  at  $t$  corresponds to  $I_{cage}(t)$ , respectively. The amount of ligand L in **Int** at  $t$  is thus expressed by  $I_L(0) - I_L(t) - I_{cage}(t)$ .

$\langle c \rangle$

The total amount of Py\* corresponds to  $I_M(0)$ . The amount of free Py\* at  $t$  corresponds to  $I_{Py^*}(t)$ . The amount of Py\* in  $[PdPy^*_4]^{2+}$  at  $t$  corresponds to  $I_M(t)$ . The amount of Py\* in **Int** at  $t$  is thus expressed by  $I_M(0) - I_{Py^*}(t) - I_M(t)$ .

The  $\langle n \rangle$  and  $\langle k \rangle$  values are determined with these  $\langle a \rangle$ ,  $\langle b \rangle$ , and  $\langle c \rangle$  values by eqs. (S1) and (S2).

$$\langle n \rangle = \frac{4 \langle a \rangle - \langle c \rangle}{\langle b \rangle} \quad (S1)$$

$$\langle k \rangle = \frac{\langle a \rangle}{\langle b \rangle} \quad (S2)$$

<sup>1</sup>H NMR spectra for the self-assembly of [Pd<sub>6</sub>L<sub>12</sub>](BF<sub>4</sub>)<sub>12</sub> complexes

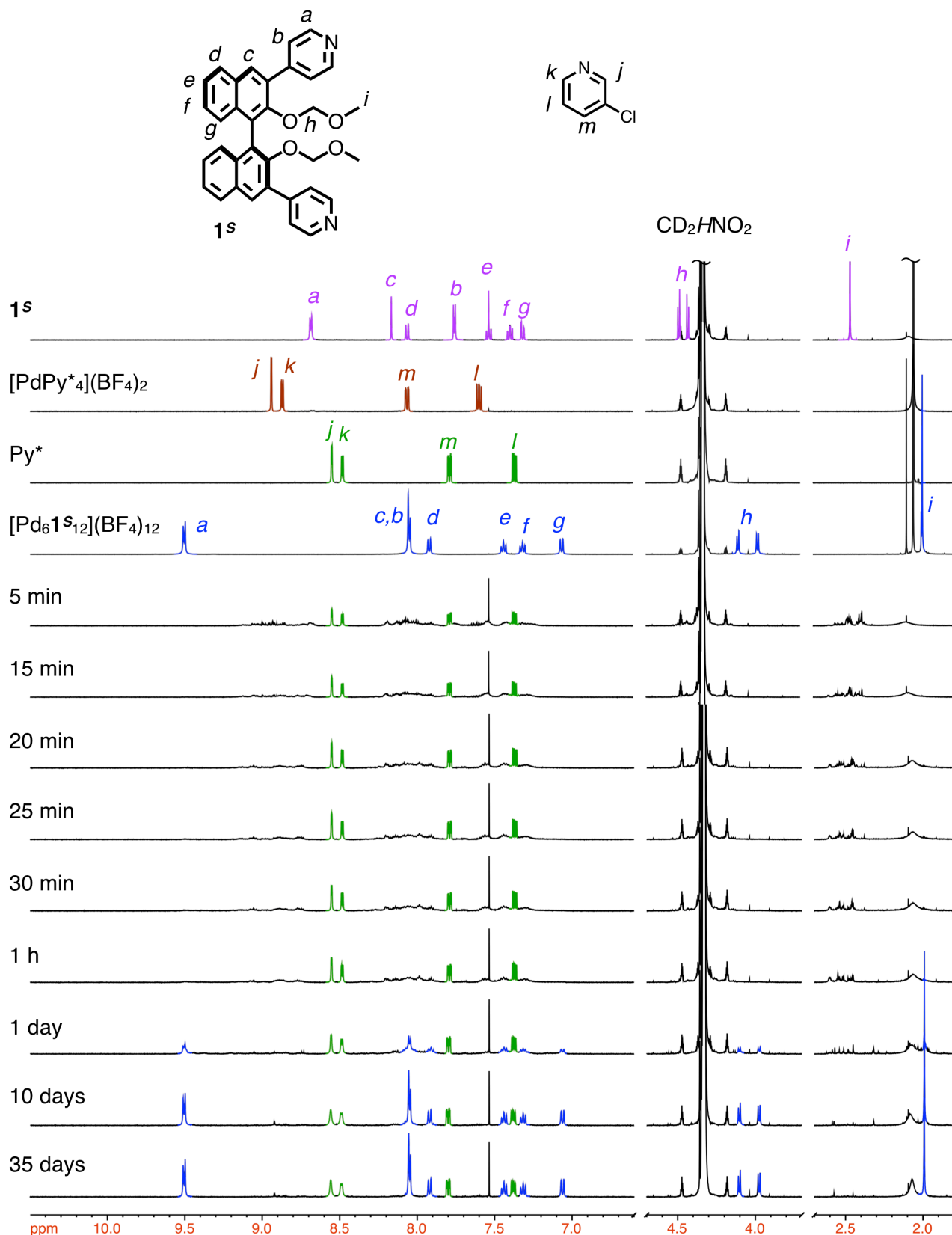


**Figure S1.** <sup>1</sup>H NMR spectra (500 MHz, CD<sub>3</sub>NO<sub>2</sub>, 298 K) of the reaction mixture for the self-assembly of [Pd<sub>6</sub>**1s**<sub>12</sub>](BF<sub>4</sub>)<sub>12</sub> from **1s** and [PdPy\*<sub>4</sub>](BF<sub>4</sub>)<sub>2</sub> at 298 K ([Pd]<sub>0</sub> = 0.95 mM and [**1s**]<sub>0</sub> = 1.9 mM). The signals colored in purple, brown, blue, and green indicate free **1s**, [PdPy\*<sub>4</sub>](BF<sub>4</sub>)<sub>2</sub>, [Pd<sub>6</sub>**1s**<sub>12</sub>](BF<sub>4</sub>)<sub>12</sub>, and Py\*, respectively.

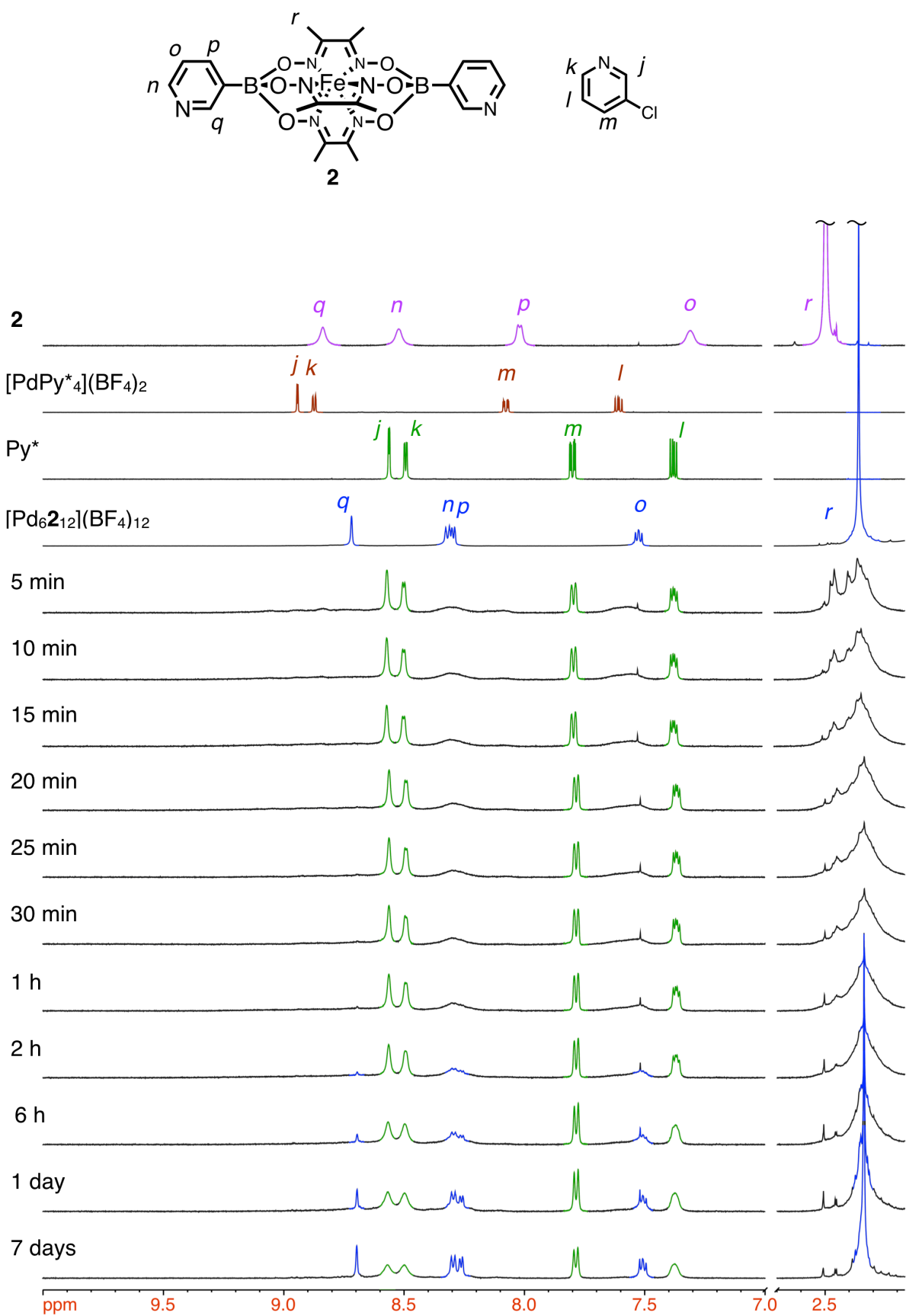


**Figure S2.** <sup>1</sup>H NMR spectra (500 MHz, CD<sub>3</sub>NO<sub>2</sub> and CD<sub>2</sub>Cl<sub>2</sub> (4:1, v/v), 298 K) of the reaction mixture for the self-assembly of [Pd<sub>6</sub>**2**<sub>12</sub>](BF<sub>4</sub>)<sub>12</sub> from **2** and [PdPy\*<sub>4</sub>](BF<sub>4</sub>)<sub>2</sub> at 298 K ([Pd]<sub>0</sub> = 1.1 mM and [b2]0 = 2.1 mM). The signals colored in purple, brown, blue, and green indicate free **2**, [PdPy\*<sub>4</sub>](BF<sub>4</sub>)<sub>2</sub>, [Pd<sub>6</sub>**2**<sub>12</sub>](BF<sub>4</sub>)<sub>12</sub>, and Py\*, respectively.

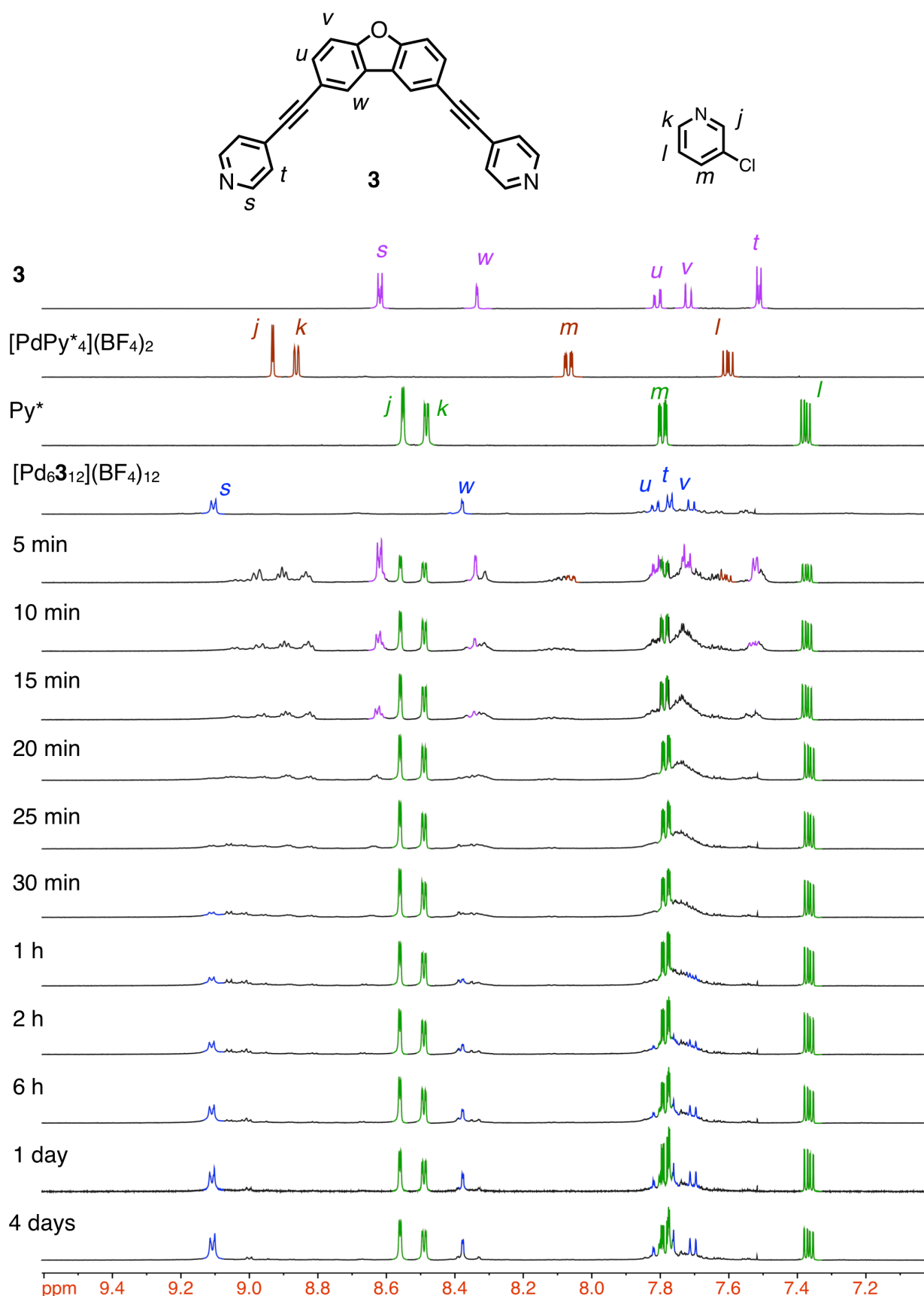


**Figure S3.** <sup>1</sup>H NMR spectra (500 MHz, CD<sub>3</sub>NO<sub>2</sub> and CD<sub>2</sub>Cl<sub>2</sub> (4:1, v/v), 298 K, aromatic region) of the reaction mixture for the self-assembly of [Pd<sub>6</sub>3<sub>12</sub>](BF<sub>4</sub>)<sub>12</sub> from **3** and [PdPy\*<sub>4</sub>](BF<sub>4</sub>)<sub>2</sub> at 298 K ([Pd]<sub>0</sub> = 1.1 mM and [3]<sub>0</sub> = 2.2 mM). The signals colored in purple, brown, blue, and green indicate free **3**, [PdPy\*<sub>4</sub>](BF<sub>4</sub>)<sub>2</sub>, [Pd<sub>6</sub>3<sub>12</sub>](BF<sub>4</sub>)<sub>12</sub>, and Py\*, respectively.



**Table S2.** Standard errors for each time point of **1<sup>s</sup>**, [PdPy\*<sub>4</sub>](BF<sub>4</sub>)<sub>2</sub>, [Pd<sub>6</sub>**1<sup>S</sup>**<sub>12</sub>](BF<sub>4</sub>)<sub>12</sub>, Py\*, and **Int**;  $\langle a \rangle$ – $\langle c \rangle$  values of the average composition of the intermediates ( $[\text{Pd}_{\langle a \rangle} \mathbf{1}^S_{\langle b \rangle} \text{Py}^*_{\langle c \rangle}]^{2\langle a \rangle +}$ ); ( $\langle n \rangle$ ,  $\langle k \rangle$ ) values for the self-assembly of [Pd<sub>6</sub>**1<sup>S</sup>**<sub>12</sub>](BF<sub>4</sub>)<sub>12</sub> from **1<sup>s</sup>** and [PdPy\*<sub>4</sub>](BF<sub>4</sub>)<sub>2</sub> in CD<sub>3</sub>NO<sub>2</sub> at 298 K ( $[\mathbf{1}^S]_0 = ca. 1.9 \text{ mM}$ ).

Time / min	<b>1<sup>s</sup></b> / %	[PdPy* <sub>4</sub> ] <sup>2+</sup> / %	[Pd <sub>6</sub> <b>1<sup>S</sup></b> <sub>12</sub> ] <sup>12+</sup> / %	Py* / %	<b>Int</b> / %	$\langle a \rangle$	$\langle b \rangle$	$\langle c \rangle$	$\langle n \rangle$	$\langle k \rangle$
0	0	0	0.00	0.00	0.00	—	—	—	—	—
5	0	0	0.00	0.72	0.00	0.005	0.010	0.012	0.014	0.000
10	0	0	0.00	1.09	0.00	0.005	0.010	0.014	0.022	0.000
15	0	0	0.00	0.51	0.00	0.005	0.010	0.004	0.010	0.000
20	0	0	0.00	1.12	0.00	0.005	0.010	0.012	0.022	0.000
25	0	0	0.00	1.40	0.00	0.005	0.010	0.015	0.028	0.000
30	0	0	0.00	1.20	0.00	0.005	0.010	0.012	0.024	0.000
35	0	0	0.00	1.62	0.00	0.005	0.010	0.016	0.032	0.000
40	0	0	0.00	0.96	0.00	0.005	0.010	0.009	0.019	0.000
45	0	0	0.00	0.75	0.00	0.005	0.010	0.006	0.015	0.000
50	0	0	0.00	1.13	0.00	0.005	0.010	0.011	0.023	0.000
55	0	0	0.00	1.03	0.00	0.005	0.010	0.009	0.021	0.000
60	0	0	0.96	0.76	0.96	0.004	0.008	0.007	0.016	0.000
120	0	0	1.20	2.08	1.20	0.002	0.003	0.019	0.044	0.000
180	0	0	0.32	0.89	0.32	0.004	0.009	0.008	0.020	0.000
240	0	0	0.21	0.65	0.21	0.005	0.009	0.006	0.016	0.000
300	0	0	1.20	0.84	1.20	0.007	0.014	0.008	0.020	0.000
360	0	0	0.28	1.33	0.28	0.004	0.008	0.013	0.033	0.000
420	0	0	0.76	0.71	0.76	0.005	0.011	0.007	0.018	0.000
480	0	0	1.05	0.80	1.05	0.006	0.013	0.008	0.021	0.000
540	0	0	0.71	1.01	0.71	0.005	0.010	0.010	0.026	0.000
720	0	0	0.66	0.83	0.66	0.005	0.010	0.007	0.024	0.000
1440	0	0	1.24	1.35	1.24	0.006	0.011	0.012	0.050	0.000
2160	0	0	1.67	0.78	1.67	0.006	0.012	0.007	0.036	0.000
2880	0	0	2.53	0.43	2.53	0.008	0.016	0.004	0.027	0.000
3600	0	0	3.19	0.46	3.19	0.009	0.018	0.004	0.022	0.000
4320	0	0	3.08	0.27	3.08	0.009	0.018	0.003	0.016	0.000
5040	0	0	3.09	0.28	3.09	0.009	0.018	0.003	0.028	0.000
5760	0	0	2.14	0.40	2.14	0.007	0.013	0.004	0.031	0.000
6480	0	0	2.47	0.29	2.47	0.007	0.014	0.003	0.028	0.000
14400	0	0	2.93	0.39	2.93	0.007	0.015	0.004	0.058	0.000
20160	0	0	2.57	0.23	2.57	0.006	0.013	0.002	0.057	0.000
30240	0	0	2.94	0.27	2.94	0.007	0.015	0.002	0.092	0.000
40320	0	0	2.89	0.06	2.89	0.007	0.014	0.001	0.068	0.000
50400	0	0	2.20	0.06	2.20	0.005	0.011	0.001	0.060	0.000









**Table S7.** Standard errors for each time point of **2**,  $[\text{PdPy}^*{}_4](\text{BF}_4)_2$ ,  $[\text{Pd}_6\mathbf{2}_{12}](\text{BF}_4)_{12}$ , Py\*, and **Int**;  $\langle a \rangle$ – $\langle c \rangle$  values of the average composition of the intermediates ( $[\text{Pd}_{\langle a \rangle}\mathbf{2}_{\langle b \rangle}\text{Py}^*_{\langle c \rangle}]^{2\langle a \rangle+}$ ); ( $\langle n \rangle$ ,  $\langle k \rangle$ ) values for the self-assembly of  $[\text{Pd}_6\mathbf{2}_{12}](\text{BF}_4)_{12}$  from **2** and  $[\text{PdPy}^*{}_4](\text{BF}_4)_2$  in  $\text{CD}_3\text{NO}_2$  and  $\text{CD}_2\text{Cl}_2$  (4:1, v/v) at 298 K ( $[\mathbf{2}]_0 = ca.\ 2.2\ \text{mM}$ )

Time / min	<b>2</b> / %	$[\text{PdPy}^*{}_4]^{2+}$ / %	$[\text{Pd}_6\mathbf{2}_{12}]^{12+}$ / %	Py* / %	<b>Int</b> / %	$\langle a \rangle$	$\langle b \rangle$	$\langle c \rangle$	$\langle n \rangle$	$\langle k \rangle$
0	0	0	0.00	0.00	0.00	—	—	—	—	—
5	0	0	0.00	3.11	0.00	0.015	0.029	0.047	0.062	0.000
10	0	0	0.00	4.45	0.00	0.015	0.029	0.058	0.089	0.000
15	0	0	1.39	4.59	1.39	0.017	0.034	0.059	0.091	0.000
20	0	0	1.64	2.36	1.64	0.013	0.027	0.031	0.049	0.000
25	0	0	1.60	0.37	1.60	0.012	0.025	0.004	0.007	0.000
30	0	0	1.77	0.20	1.77	0.012	0.025	0.002	0.004	0.000
35	0	0	2.02	0.52	2.02	0.010	0.021	0.005	0.011	0.000
40	0	0	1.12	0.43	1.12	0.012	0.024	0.005	0.009	0.000
45	0	0	0.89	0.38	0.89	0.011	0.023	0.004	0.008	0.000
50	0	0	1.65	1.38	1.65	0.009	0.018	0.015	0.029	0.000
55	0	0	1.36	0.21	1.36	0.010	0.019	0.002	0.004	0.000
60	0	0	1.05	0.51	1.05	0.010	0.021	0.005	0.011	0.000
120	0	0	2.01	0.55	2.01	0.007	0.014	0.006	0.012	0.000
180	0	0	3.84	0.65	3.84	0.001	0.002	0.007	0.015	0.000
240	0	0	5.94	0.70	5.94	0.006	0.012	0.008	0.016	0.000
300	0	0	5.97	0.66	5.97	0.006	0.012	0.007	0.016	0.000
360	0	0	6.05	0.87	6.05	0.007	0.014	0.009	0.019	0.000
720	0	0	8.93	1.00	8.93	0.017	0.033	0.011	0.026	0.000
1440	0	0	10.18	0.63	10.18	0.022	0.044	0.007	0.021	0.000
2880	0	0	9.55	0.95	9.55	0.022	0.044	0.011	0.046	0.000
4320	0	0	5.63	0.35	5.63	0.011	0.023	0.004	0.017	0.000
5760	0	0	3.53	0.35	3.53	0.006	0.011	0.004	0.018	0.000
7200	0	0	2.86	0.35	2.86	0.004	0.008	0.004	0.019	0.000
10080	0	0	2.92	0.35	2.92	0.004	0.008	0.004	0.019	0.000

**Table S8.** Time variation of **2**, [PdPy\*<sub>4</sub>](BF<sub>4</sub>)<sub>2</sub>, [Pd<sub>6</sub>**2**<sub>12</sub>](BF<sub>4</sub>)<sub>12</sub>, Py\*, and Int;  $\langle a \rangle$ – $\langle c \rangle$  values of the average composition of the intermediates ([Pd<sub>(a)</sub>**2**<sub>(b)</sub>Py\*<sub>(c)</sub>]<sup>2+<sub>(a)</sub></sup>); ( $\langle n \rangle$ ,  $\langle k \rangle$ ) values for the self-assembly of [Pd<sub>6</sub>**2**<sub>12</sub>](BF<sub>4</sub>)<sub>12</sub> from **2** and [PdPy\*<sub>4</sub>](BF<sub>4</sub>)<sub>2</sub> in CD<sub>3</sub>NO<sub>2</sub> and CD<sub>2</sub>Cl<sub>2</sub> (4:1, v/v) at 298 K ([**2**]<sub>0</sub> = 2.1 mM). (run 4)

Time / min	<b>2</b> / %	[PdPy* <sub>4</sub> ] <sup>2+</sup> / %	[Pd <sub>6</sub> <b>2</b> <sub>12</sub> ] <sup>12+</sup> / %	Py* / %	Int / %	$\langle a \rangle$	$\langle b \rangle$	$\langle c \rangle$	$\langle n \rangle$	$\langle k \rangle$
0	100.0	100.0	0.0	0.0	0.0	—	—	—	—	—
5	0.0	0.0	0.0	86.1	100.0	0.270	0.540	0.150	1.722	0.500
10	0.0	0.0	0.0	97.8	100.0	0.270	0.540	0.024	1.956	0.500
15	0.0	0.0	4.2	98.9	95.8	0.259	0.518	0.012	1.976	0.500
20	0.0	0.0	5.4	97.8	94.6	0.255	0.511	0.024	1.954	0.500
25	0.0	0.0	4.6	99.7	95.4	0.257	0.515	0.003	1.994	0.500
30	0.0	0.0	5.4	99.1	94.6	0.255	0.511	0.010	1.981	0.500
35	0.0	0.0	4.6	97.8	95.4	0.257	0.515	0.024	1.954	0.500
40	0.0	0.0	6.1	99.1	93.9	0.254	0.507	0.010	1.980	0.500
45	0.0	0.0	5.4	99.3	94.6	0.255	0.511	0.008	1.985	0.500
50	0.0	0.0	4.2	99.9	95.8	0.259	0.517	0.001	1.999	0.500
55	0.0	0.0	5.5	99.9	94.5	0.255	0.510	0.001	1.999	0.500
60	0.0	0.0	6.9	98.7	93.1	0.251	0.503	0.014	1.971	0.500
120	0.0	0.0	8.9	98.0	91.1	0.246	0.492	0.021	1.957	0.500
180	0.0	0.0	9.4	99.9	90.6	0.244	0.489	0.001	1.999	0.500
240	0.0	0.0	11.6	100.6	88.4	0.239	0.478	-0.006	2.013	0.500
300	0.0	0.0	13.5	98.7	86.5	0.233	0.467	0.014	1.969	0.500
360	0.0	0.0	16.9	99.1	83.1	0.224	0.449	0.010	1.978	0.500
720	0.0	0.0	21.0	100.8	79.0	0.213	0.427	-0.009	2.020	0.500
1440	0.0	0.0	30.6	99.5	69.4	0.187	0.375	0.005	1.986	0.500
2880	0.0	0.0	44.4	98.9	55.6	0.150	0.301	0.012	1.959	0.500
4320	0.0	0.0	57.4	98.9	42.6	0.115	0.230	0.012	1.947	0.500
5760	0.0	0.0	61.0	98.9	39.0	0.105	0.211	0.012	1.942	0.500
7200	0.0	0.0	62.8	98.9	37.2	0.100	0.201	0.012	1.939	0.500
10080	0.0	0.0	62.5	98.9	37.5	0.101	0.203	0.012	1.940	0.500

**Table S9.** Time variation of **2**,  $[\text{PdPy}^*_4](\text{BF}_4)_2$ ,  $[\text{Pd}_6\mathbf{2}_{12}](\text{BF}_4)_{12}$ ,  $\text{Py}^*$ , and **Int**;  $\langle a \rangle - \langle c \rangle$  values of the average composition of the intermediates ( $[\text{Pd}_{\langle a \rangle} \mathbf{2}_{\langle b \rangle} \text{Py}^*]^{2\langle a \rangle +}$ ); ( $\langle n \rangle$ ,  $\langle k \rangle$ ) values for the self-assembly of  $[\text{Pd}_6\mathbf{2}_{12}](\text{BF}_4)_{12}$  from **2** and  $[\text{PdPy}^*_4](\text{BF}_4)_2$  in  $\text{CD}_3\text{NO}_2$  and  $\text{CD}_2\text{Cl}_2$  (4:1, v/v) at 298 K ( $[\mathbf{2}]_0 = 2.1$  mM). (run 5)

Time / min	<b>2</b> / %	$[\text{PdPy}^*_4]^{2+}$ / %	$[\text{Pd}_6\mathbf{2}_{12}]^{12+}$ / %	$\text{Py}^*$ / %	<b>Int</b> / %	$\langle a \rangle$	$\langle b \rangle$	$\langle c \rangle$	$\langle n \rangle$	$\langle k \rangle$
0	100.0	100.0	0.0	0.0	0.0	—	—	—	—	—
5	0.0	0.0	0.0	87.6	100.0	0.273	0.545	0.135	1.753	0.500
10	0.0	0.0	0.0	92.1	100.0	0.273	0.545	0.087	1.841	0.500
15	0.0	0.0	0.0	93.7	100.0	0.273	0.545	0.068	1.875	0.500
20	0.0	0.0	0.0	96.1	100.0	0.273	0.545	0.043	1.921	0.500
25	0.0	0.0	0.0	98.8	100.0	0.273	0.545	0.013	1.976	0.500
30	0.0	0.0	0.0	98.8	100.0	0.273	0.545	0.013	1.976	0.500
35	0.0	0.0	0.0	98.2	100.0	0.273	0.545	0.020	1.963	0.500
40	0.0	0.0	3.1	98.6	96.9	0.264	0.528	0.015	1.971	0.500
45	0.0	0.0	4.4	98.2	95.6	0.261	0.521	0.020	1.962	0.500
50	0.0	0.0	5.4	96.3	94.6	0.258	0.516	0.041	1.921	0.500
55	0.0	0.0	5.4	99.2	94.6	0.258	0.516	0.008	1.984	0.500
60	0.0	0.0	6.9	97.8	93.1	0.254	0.508	0.025	1.952	0.500
120	0.0	0.0	9.6	97.8	90.4	0.246	0.493	0.025	1.950	0.500
180	0.0	0.0	10.5	97.8	89.5	0.244	0.488	0.025	1.950	0.500
240	0.0	0.0	11.4	98.2	88.6	0.242	0.483	0.020	1.959	0.500
300	0.0	0.0	12.8	98.6	87.2	0.238	0.476	0.015	1.968	0.500
360	0.0	0.0	13.4	96.7	86.6	0.236	0.472	0.036	1.924	0.500
720	0.0	0.0	19.2	97.3	80.8	0.220	0.441	0.029	1.934	0.500
1440	0.0	0.0	29.3	97.3	70.7	0.193	0.386	0.029	1.925	0.500
2880	0.0	0.0	42.1	98.0	57.9	0.158	0.316	0.022	1.930	0.500
4320	0.0	0.0	53.9	99.2	46.1	0.126	0.252	0.008	1.966	0.500
5760	0.0	0.0	62.4	99.2	37.6	0.103	0.205	0.008	1.959	0.500
7200	0.0	0.0	64.9	99.2	35.1	0.096	0.192	0.008	1.956	0.500
10080	0.0	0.0	65.0	99.2	35.0	0.096	0.191	0.008	1.956	0.500

**Table S10.** Time variation of **2**,  $[\text{PdPy}^*_4](\text{BF}_4)_2$ ,  $[\text{Pd}_6\mathbf{2}_{12}](\text{BF}_4)_{12}$ , Py\*, and **Int**;  $\langle a \rangle - \langle c \rangle$  values of the average composition of the intermediates ( $[\text{Pd}_{\langle a \rangle}\mathbf{2}_{\langle b \rangle}\text{Py}^*]^{2\langle a \rangle+}$ ); ( $\langle n \rangle$ ,  $\langle k \rangle$ ) values for the self-assembly of  $[\text{Pd}_6\mathbf{2}_{12}](\text{BF}_4)_{12}$  from **2** and  $[\text{PdPy}^*_4](\text{BF}_4)_2$  in  $\text{CD}_3\text{NO}_2$  and  $\text{CD}_2\text{Cl}_2$  (4:1, v/v) at 298 K ( $[\mathbf{2}]_0 = 2.4$  mM). (run 6)

Time / min	<b>2</b> / %	$[\text{PdPy}^*_4]^{2+}$ / %	$[\text{Pd}_6\mathbf{2}_{12}]^{12+}$ / %	Py* / %	<b>Int</b> / %	$\langle a \rangle$	$\langle b \rangle$	$\langle c \rangle$	$\langle n \rangle$	$\langle k \rangle$
0	100.0	100.0	0.0	0.0	0.0	—	—	—	—	—
5	0.0	0.0	0.0	77.6	100.0	0.315	0.630	0.282	1.553	0.500
10	0.0	0.0	0.0	82.6	100.0	0.315	0.630	0.220	1.651	0.500
15	0.0	0.0	0.0	83.3	100.0	0.315	0.630	0.211	1.666	0.500
20	0.0	0.0	4.3	90.0	95.7	0.302	0.603	0.126	1.792	0.500
25	0.0	0.0	5.0	100.1	95.0	0.299	0.599	-0.001	2.001	0.500
30	0.0	0.0	5.3	99.5	94.7	0.298	0.597	0.006	1.990	0.500
35	0.0	0.0	6.9	99.5	93.1	0.293	0.587	0.006	1.989	0.500
40	0.0	0.0	6.7	100.1	93.3	0.294	0.588	-0.001	2.001	0.500
45	0.0	0.0	7.4	99.3	92.6	0.292	0.583	0.009	1.985	0.500
50	0.0	0.0	9.7	100.8	90.3	0.285	0.569	-0.010	2.017	0.500
55	0.0	0.0	9.5	99.5	90.5	0.285	0.570	0.006	1.989	0.500
60	0.0	0.0	10.0	99.5	90.0	0.284	0.567	0.006	1.989	0.500
120	0.0	0.0	15.2	99.5	84.8	0.267	0.534	0.006	1.988	0.500
180	0.0	0.0	21.4	98.4	78.6	0.248	0.495	0.020	1.960	0.500
240	0.0	0.0	29.3	99.7	70.7	0.223	0.446	0.004	1.991	0.500
300	0.0	0.0	31.0	100.6	69.0	0.217	0.435	-0.008	2.017	0.500
360	0.0	0.0	33.0	99.5	67.0	0.211	0.422	0.006	1.985	0.500
720	0.0	0.0	46.8	98.8	53.2	0.168	0.335	0.015	1.954	0.500
1440	0.0	0.0	60.5	98.4	39.5	0.125	0.249	0.020	1.920	0.500
2880	0.0	0.0	71.8	101.1	28.2	0.089	0.178	-0.014	2.081	0.500
4320	0.0	0.0	72.2	100.1	27.8	0.088	0.175	-0.001	2.004	0.500
5760	0.0	0.0	72.2	100.1	27.8	0.088	0.175	-0.001	2.004	0.500
7200	0.0	0.0	72.2	100.1	27.8	0.088	0.175	-0.001	2.004	0.500
10080	0.0	0.0	72.2	100.1	27.8	0.088	0.175	-0.001	2.004	0.500

**Table S11.** Average time variation of **3**,  $[\text{PdPy}^*_4](\text{BF}_4)_2$ ,  $[\text{Pd}_6\mathbf{3}_{12}](\text{BF}_4)_{12}$ , Py\*, and **Int**;  $\langle a \rangle$ – $\langle c \rangle$  values of the average composition of the intermediates ( $[\text{Pd}_{\langle a \rangle}\mathbf{3}_{\langle b \rangle}\text{Py}^*_{\langle c \rangle}]^{2\langle a \rangle+}$ ); ( $\langle n \rangle$ ,  $\langle k \rangle$ ) values for the self-assembly of  $[\text{Pd}_6\mathbf{3}_{12}](\text{BF}_4)_{12}$  from **3** and  $[\text{PdPy}^*_4](\text{BF}_4)_2$  in  $\text{CD}_3\text{NO}_2$  and  $\text{CD}_2\text{Cl}_2$  (4:1, v/v) at 298 K ( $[\mathbf{3}]_0 = ca. 2.2 \text{ mM}$ ).

Time / min	<b>3</b> / %	$[\text{PdPy}^*_4]^{2+}$ / %	$[\text{Pd}_6\mathbf{3}_{12}]^{12+}$ / %	Py* / %	<b>Int</b> / %	$\langle a \rangle$	$\langle b \rangle$	$\langle c \rangle$	$\langle n \rangle$	$\langle k \rangle$
0	100.0	100.0	0.0	0.0	0.0	—	—	—	—	—
5	38.5	14.1	1.4	50.6	60.0	0.242	0.344	0.401	1.634	0.706
10	19.3	4.3	2.8	72.2	77.9	0.266	0.446	0.267	1.782	0.596
15	12.6	3.2	4.0	80.5	83.4	0.266	0.478	0.184	1.834	0.556
20	10.4	2.9	5.1	86.1	84.5	0.263	0.484	0.124	1.915	0.544
25	7.6	2.5	6.0	88.0	86.5	0.262	0.495	0.107	1.897	0.530
30	7.0	2.3	6.6	90.4	86.4	0.261	0.495	0.082	1.941	0.528
35	6.4	1.9	7.3	91.7	86.3	0.260	0.494	0.072	1.956	0.527
40	5.7	2.4	8.0	91.9	86.3	0.256	0.495	0.064	1.942	0.519
45	5.6	2.5	8.4	91.9	86.0	0.255	0.493	0.062	1.943	0.518
50	5.3	1.7	9.0	92.6	85.7	0.256	0.491	0.064	1.950	0.522
55	5.2	2.5	9.5	93.4	85.2	0.252	0.489	0.046	1.966	0.516
60	5.1	2.5	10.3	93.6	84.6	0.250	0.485	0.044	1.967	0.515
120	4.4	2.5	14.1	93.9	81.5	0.239	0.467	0.039	1.957	0.512
180	3.4	2.0	17.0	94.2	79.6	0.232	0.457	0.042	1.941	0.510
240	3.3	2.0	20.3	94.6	76.4	0.223	0.438	0.038	1.946	0.509
300	3.1	2.0	23.0	94.7	73.9	0.215	0.424	0.037	1.940	0.508
360	3.0	2.0	25.5	94.8	71.5	0.208	0.410	0.036	1.938	0.508
720	2.7	1.6	32.5	95.8	64.8	0.189	0.372	0.029	1.952	0.510
1440	2.4	1.6	41.0	96.4	56.7	0.165	0.326	0.022	1.950	0.509
2880	2.3	1.6	46.8	96.0	50.8	0.148	0.292	0.026	1.929	0.508
4320	2.3	1.7	48.7	96.1	49.1	0.142	0.281	0.024	1.930	0.506
5760	2.1	1.7	48.8	96.0	49.1	0.142	0.281	0.025	1.921	0.504

**Table S12.** Standard errors for each time point of **3**, [PdPy<sup>\*</sup><sub>4</sub>](BF<sub>4</sub>)<sub>2</sub>, [Pd<sub>6</sub>**3**<sub>12</sub>](BF<sub>4</sub>)<sub>12</sub>, Py\*, and **Int**;  $\langle a \rangle$ – $\langle c \rangle$  values of the average composition of the intermediates ( $[\text{Pd}_{\langle a \rangle}\mathbf{3}_{\langle b \rangle}\text{Py}^*_{\langle c \rangle}]^{2\langle a \rangle+}$ ); ( $\langle n \rangle$ ,  $\langle k \rangle$ ) values for the self-assembly of [Pd<sub>6</sub>**3**<sub>12</sub>](BF<sub>4</sub>)<sub>12</sub> from **3** and [PdPy<sup>\*</sup><sub>4</sub>](BF<sub>4</sub>)<sub>2</sub> in CD<sub>3</sub>NO<sub>2</sub> and CD<sub>2</sub>Cl<sub>2</sub> (4:1, v/v) at 298 K ([**3**]<sub>0</sub> = ca. 2.2 mM)

Time / min	<b>3</b> / %	[PdPy <sup>*</sup> <sub>4</sub> ] <sup>2+</sup> / %	[Pd <sub>6</sub> <b>3</b> <sub>12</sub> ] <sup>12+</sup> / %	Py* / %	<b>Int</b> / %	$\langle a \rangle$	$\langle b \rangle$	$\langle c \rangle$	$\langle n \rangle$	$\langle k \rangle$
0	0.00	0.00	0.00	0.00	0.00	—	—	—	—	—
5	2.80	1.08	0.06	4.29	2.75	0.006	0.023	0.036	0.075	0.028
10	0.34	0.48	0.06	3.34	0.30	0.006	0.013	0.033	0.078	0.005
15	0.59	0.55	0.13	3.18	0.68	0.006	0.016	0.036	0.064	0.007
20	0.76	0.32	0.15	2.59	0.77	0.006	0.017	0.028	0.048	0.006
25	1.37	0.28	0.32	2.46	1.46	0.007	0.020	0.024	0.030	0.008
30	1.18	0.05	0.37	2.64	1.34	0.008	0.020	0.028	0.035	0.007
35	1.23	0.62	0.57	2.41	1.59	0.007	0.022	0.027	0.030	0.009
40	1.17	0.32	0.62	2.31	1.36	0.008	0.020	0.024	0.031	0.007
45	1.19	0.26	0.66	2.38	1.41	0.008	0.021	0.025	0.033	0.007
50	1.20	0.69	0.82	2.34	1.46	0.008	0.021	0.028	0.037	0.007
55	1.17	0.26	0.82	2.17	1.57	0.008	0.021	0.023	0.031	0.007
60	1.19	0.26	0.96	1.87	1.54	0.008	0.021	0.020	0.026	0.007
120	0.88	0.26	1.68	1.99	2.26	0.010	0.025	0.021	0.030	0.005
180	1.05	0.52	2.69	1.72	3.68	0.012	0.032	0.019	0.027	0.009
240	1.01	0.50	2.85	1.24	3.75	0.012	0.032	0.012	0.025	0.009
300	0.88	0.50	3.41	1.47	4.14	0.013	0.033	0.015	0.031	0.009
360	0.92	0.50	3.85	1.52	4.53	0.014	0.034	0.016	0.029	0.009
720	0.79	0.07	4.31	1.68	4.91	0.016	0.036	0.018	0.035	0.007
1440	0.82	0.07	5.15	1.88	5.80	0.018	0.040	0.021	0.044	0.009
2880	0.73	0.06	3.35	2.02	3.76	0.012	0.027	0.022	0.057	0.008
4320	0.66	0.05	1.82	1.49	2.19	0.007	0.018	0.016	0.037	0.007
5760	0.56	0.05	1.68	1.76	1.99	0.007	0.016	0.018	0.052	0.005

**Table S13.** Time variation of **3**, [PdPy $^*_4$ ](BF<sub>4</sub>)<sub>2</sub>, [Pd<sub>6</sub>**3**<sub>12</sub>](BF<sub>4</sub>)<sub>12</sub>, Py\*, and **Int**;  $\langle a \rangle - \langle c \rangle$  values of the average composition of the intermediates ([Pd<sub>(a)</sub>**3**<sub>(b)</sub>Py $^{*(c)}$ ]<sup>2(a)</sup>); ( $\langle n \rangle$ ,  $\langle k \rangle$ ) values for the self-assembly of [Pd<sub>6</sub>**3**<sub>12</sub>](BF<sub>4</sub>)<sub>12</sub> from **3** and [PdPy $^*_4$ ](BF<sub>4</sub>)<sub>2</sub> in CD<sub>3</sub>NO<sub>2</sub> and CD<sub>2</sub>Cl<sub>2</sub> (4:1, v/v) at 298 K ([**3**]<sub>0</sub> = 2.3 mM). (run 7)

Time / min	<b>3</b> / %	[PdPy $^*_4$ ] <sup>2+</sup> / %	[Pd <sub>6</sub> <b>3</b> <sub>12</sub> ] <sup>12+</sup> / %	Py* / %	<b>Int</b> / %	$\langle a \rangle$	$\langle b \rangle$	$\langle c \rangle$	$\langle n \rangle$	$\langle k \rangle$
0	100.0	100.0	0.0	0.0	0.0	—	—	—	—	—
5	40.3	16.2	1.4	50.5	58.3	0.242	0.342	0.392	1.684	0.708
10	19.0	5.2	2.8	74.0	78.3	0.270	0.460	0.244	1.819	0.588
15	12.3	4.0	3.8	81.6	83.9	0.271	0.493	0.170	1.854	0.550
20	10.6	3.5	4.8	87.9	84.5	0.269	0.497	0.101	1.965	0.542
25	8.2	3.0	5.4	88.4	86.5	0.269	0.508	0.101	1.920	0.530
30	6.9	2.3	5.9	90.0	87.3	0.270	0.513	0.090	1.929	0.526
35	6.3	3.1	6.3	92.8	87.4	0.266	0.513	0.048	1.979	0.518
40	6.1	3.0	6.8	92.5	87.1	0.265	0.511	0.052	1.969	0.518
45	6.1	3.0	7.1	92.8	86.8	0.264	0.510	0.049	1.975	0.518
50	6.0	3.0	7.4	94.1	86.6	0.263	0.508	0.034	2.002	0.517
55	6.0	3.0	8.1	94.2	85.9	0.261	0.505	0.033	2.004	0.517
60	5.7	3.0	8.5	94.6	85.8	0.260	0.504	0.028	2.007	0.516
120	4.8	3.0	11.7	94.0	83.5	0.250	0.491	0.035	1.970	0.510
180	2.1	3.0	12.2	94.4	85.7	0.249	0.503	0.030	1.918	0.495
240	2.1	3.0	15.1	93.8	82.9	0.241	0.487	0.037	1.900	0.494
300	2.0	3.0	16.4	93.8	81.6	0.237	0.479	0.037	1.896	0.493
360	1.9	3.0	17.9	94.2	80.2	0.232	0.471	0.033	1.903	0.493
720	1.9	1.7	24.2	95.9	73.9	0.218	0.434	0.029	1.939	0.501
1440	1.5	1.7	31.1	98.7	67.5	0.197	0.396	-0.005	2.006	0.498
2880	1.5	1.7	40.2	97.9	58.3	0.171	0.342	0.005	1.980	0.499
4320	1.5	1.7	45.1	98.3	53.4	0.156	0.314	0.000	1.991	0.498
5760	1.4	1.7	45.5	98.0	53.1	0.155	0.312	0.004	1.976	0.497

**Table S14.** Time variation of **3**,  $[\text{PdPy}^{\ast}_4](\text{BF}_4)_2$ ,  $[\text{Pd}_6\mathbf{3}_{12}](\text{BF}_4)_{12}$ , Py $^{\ast}$ , and **Int**;  $\langle a \rangle - \langle c \rangle$  values of the average composition of the intermediates ( $[\text{Pd}_{\langle a \rangle}\mathbf{3}_{\langle b \rangle}\text{Py}^{\ast}_{\langle c \rangle}]^{2\langle a \rangle+}$ ); ( $\langle n \rangle$ ,  $\langle k \rangle$ ) values for the self-assembly of  $[\text{Pd}_6\mathbf{3}_{12}](\text{BF}_4)_{12}$  from **3** and  $[\text{PdPy}^{\ast}_4](\text{BF}_4)_2$  in  $\text{CD}_3\text{NO}_2$  and  $\text{CD}_2\text{Cl}_2$  (4:1, v/v) at 298 K ( $[\mathbf{3}]_0 = 2.2 \text{ mM}$ ). (run 8)

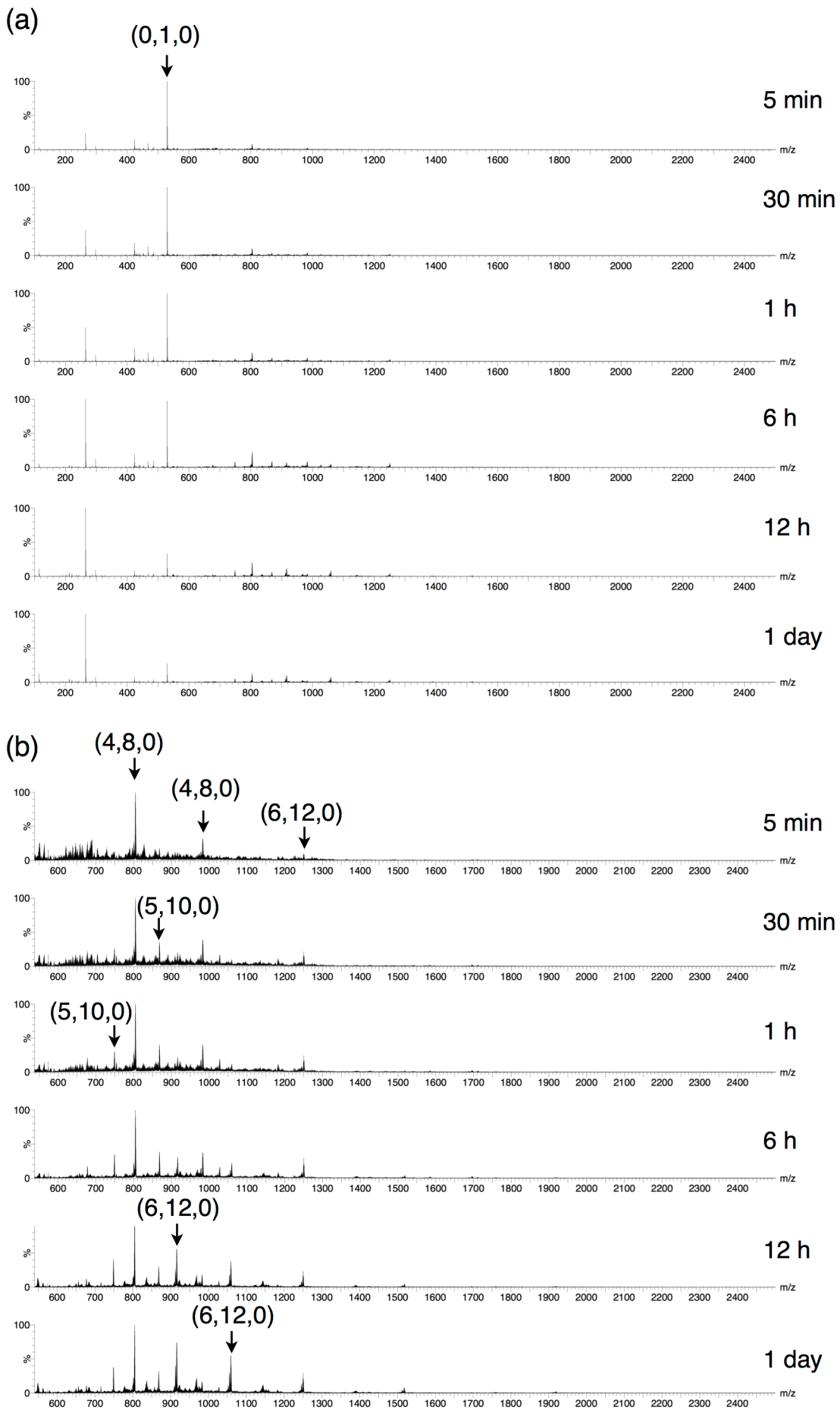
Time / min	<b>3</b> / %	$[\text{PdPy}^{\ast}_4]^{2+}$ / %	$[\text{Pd}_6\mathbf{3}_{12}]^{12+}$ / %	Py $^{\ast}$ / %	<b>Int</b> / %	$\langle a \rangle$	$\langle b \rangle$	$\langle c \rangle$	$\langle n \rangle$	$\langle k \rangle$
0	100.0	100.0	0.0	0.0	0.0	—	—	—	—	—
5	33.0	12.5	1.5	58.2	65.4	0.252	0.384	0.344	1.730	0.657
10	19.0	4.0	2.9	76.9	78.1	0.273	0.459	0.224	1.895	0.596
15	11.7	3.5	4.0	85.4	84.2	0.272	0.495	0.130	1.932	0.549
20	8.9	2.9	5.2	89.4	85.8	0.270	0.504	0.091	1.960	0.535
25	5.0	2.1	6.0	92.1	89.0	0.270	0.523	0.068	1.934	0.516
30	5.1	2.2	6.8	95.2	88.1	0.267	0.518	0.031	2.006	0.517
35	4.3	1.2	7.4	95.3	88.3	0.268	0.519	0.041	1.991	0.518
40	3.4	2.0	8.3	95.5	88.2	0.263	0.518	0.030	1.976	0.508
45	3.4	2.2	8.7	95.6	87.9	0.262	0.516	0.026	1.976	0.507
50	3.0	0.9	9.4	95.7	87.6	0.264	0.515	0.040	1.970	0.512
55	2.9	2.2	9.5	96.7	87.6	0.260	0.515	0.014	1.991	0.504
60	2.8	2.2	10.8	96.2	86.5	0.256	0.508	0.019	1.976	0.503
120	2.7	2.2	13.3	97.4	84.0	0.248	0.494	0.006	2.001	0.503
180	2.6	1.4	17.2	97.2	80.2	0.239	0.471	0.017	1.995	0.508
240	2.5	1.5	21.0	97.1	76.5	0.228	0.450	0.017	1.987	0.507
300	2.4	1.5	24.9	97.5	72.7	0.216	0.427	0.012	1.999	0.507
360	2.2	1.5	28.4	97.6	69.4	0.206	0.408	0.010	1.995	0.505
720	1.9	1.5	34.7	98.6	63.4	0.188	0.372	-0.001	2.018	0.504
1440	1.7	1.5	43.4	97.8	54.9	0.162	0.323	0.008	1.983	0.502
2880	1.7	1.5	50.6	98.1	47.7	0.141	0.280	0.004	1.992	0.502
4320	1.8	1.7	51.1	96.7	47.1	0.139	0.277	0.019	1.936	0.501
5760	1.7	1.7	51.1	97.5	47.2	0.139	0.277	0.009	1.970	0.500

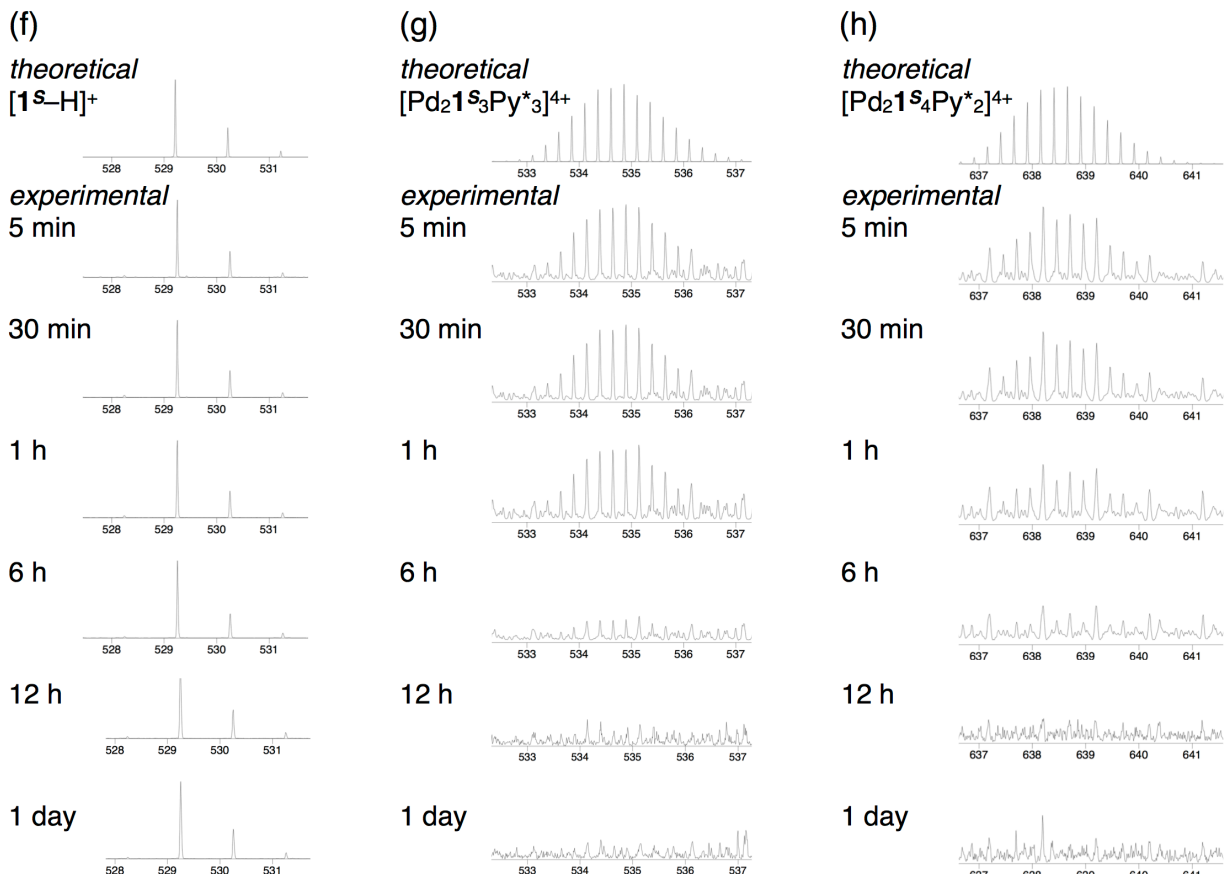
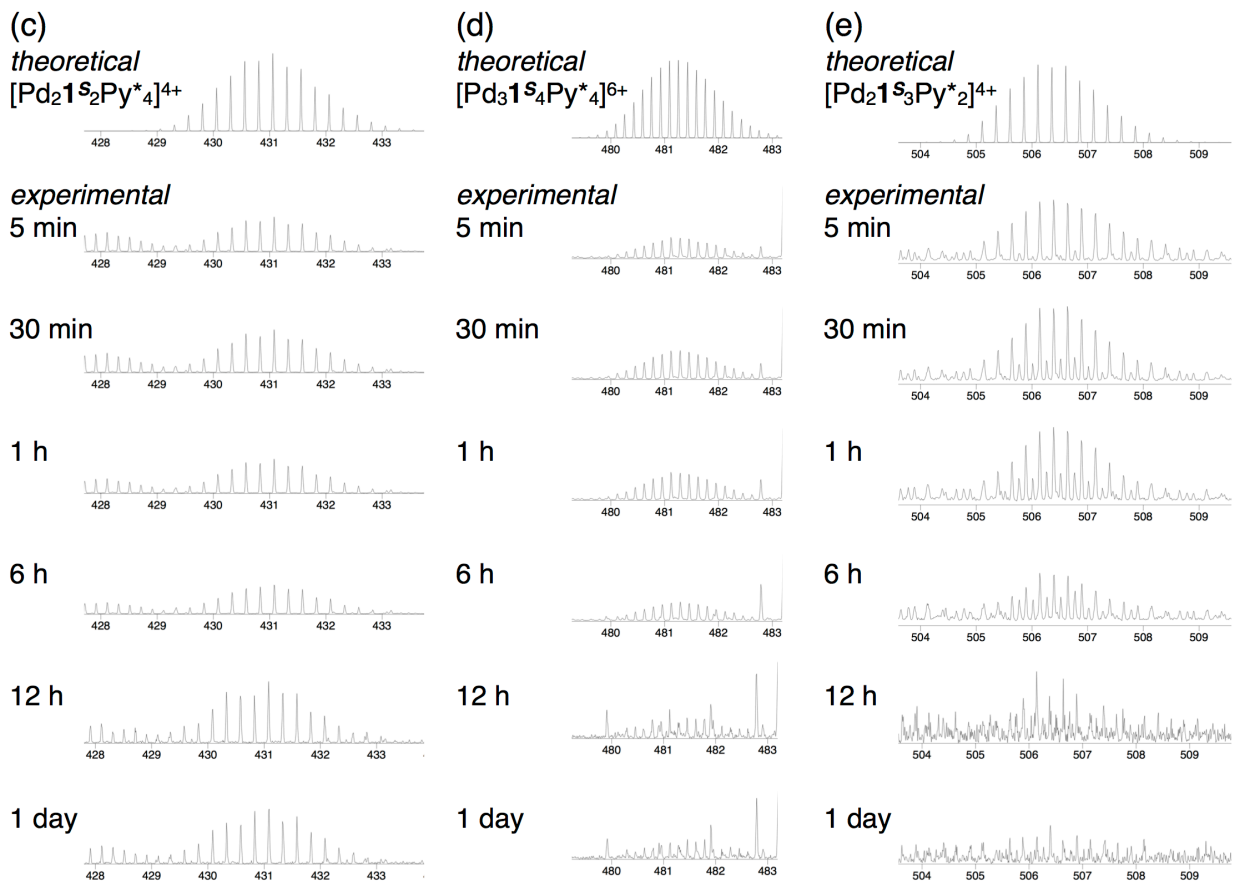
**Table S15.** Time variation of **3**,  $[\text{PdPy}^*_4](\text{BF}_4)_2$ ,  $[\text{Pd}_6\mathbf{3}_{12}](\text{BF}_4)_{12}$ , Py\*, and Int;  $\langle a \rangle - \langle c \rangle$  values of the average composition of the intermediates ( $[\text{Pd}_{\langle a \rangle}\mathbf{3}_{\langle b \rangle}\text{Py}^*_{\langle c \rangle}]^{2\langle a \rangle+}$ ); ( $\langle n \rangle$ ,  $\langle k \rangle$ ) values for the self-assembly of  $[\text{Pd}_6\mathbf{3}_{12}](\text{BF}_4)_{12}$  from **3** and  $[\text{PdPy}^*_4](\text{BF}_4)_2$  in  $\text{CD}_3\text{NO}_2$  and  $\text{CD}_2\text{Cl}_2$  (4:1, v/v) at 298 K ( $[\mathbf{3}]_0 = 2.1 \text{ mM}$ ). (run 9)

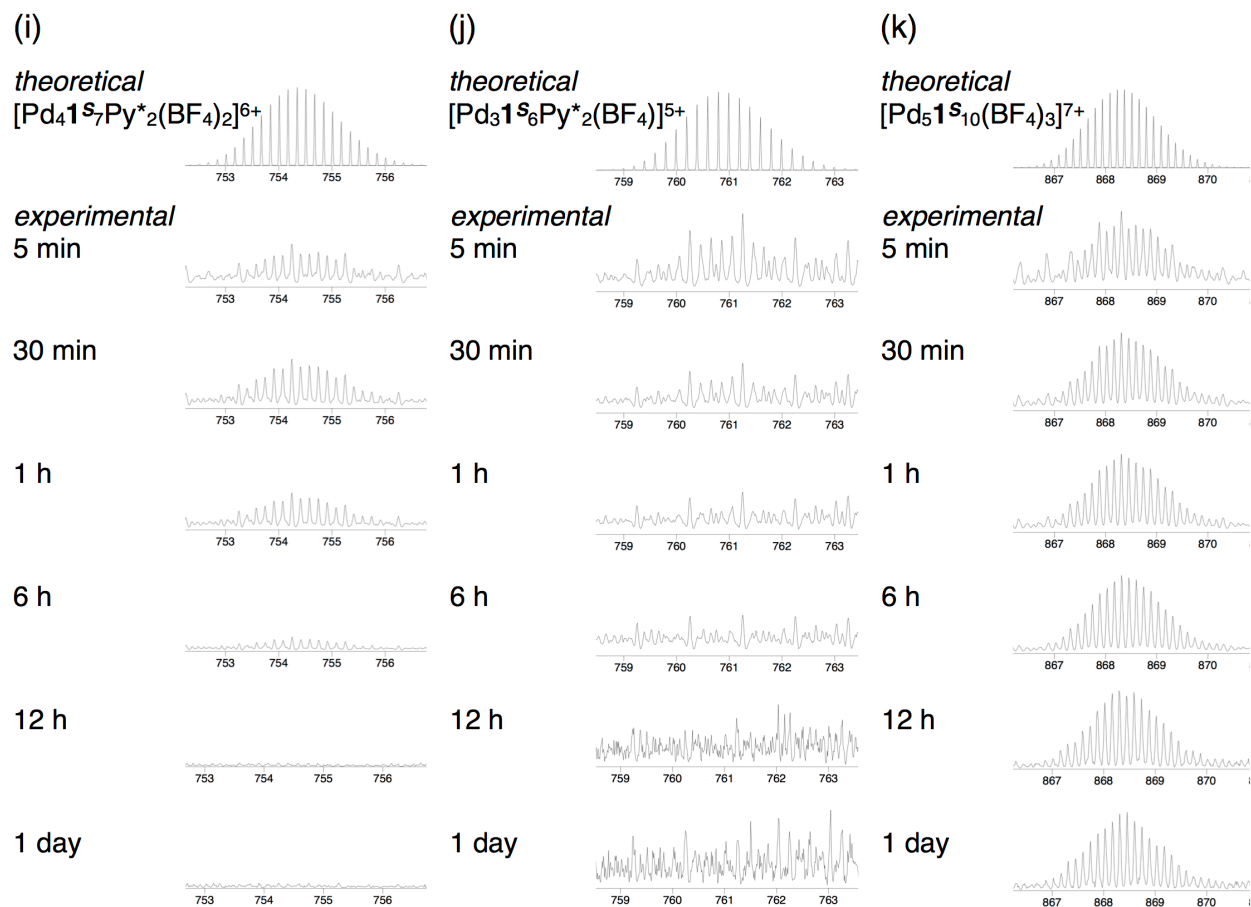
Time / min	<b>3</b> / %	$[\text{PdPy}^*_4]^{2+}$ / %	$[\text{Pd}_6\mathbf{3}_{12}]^{12+}$ / %	Py* / %	Int / %	$\langle a \rangle$	$\langle b \rangle$	$\langle c \rangle$	$\langle n \rangle$	$\langle k \rangle$
0	100.0	100.0	0.0	0.0	0.0	—	—	—	—	—
5	42.2	13.6	1.4	43.3	56.4	0.231	0.306	0.468	1.487	0.753
10	20.0	3.7	2.7	65.8	77.3	0.254	0.419	0.332	1.632	0.606
15	13.7	2.1	4.2	74.5	82.0	0.254	0.445	0.253	1.714	0.571
20	11.5	2.4	5.3	80.9	83.2	0.250	0.451	0.181	1.819	0.555
25	9.6	2.4	6.5	83.6	83.9	0.247	0.455	0.152	1.838	0.543
30	9.2	2.4	7.1	86.1	83.7	0.246	0.454	0.126	1.886	0.541
35	8.6	1.3	8.3	87.1	83.1	0.245	0.451	0.126	1.897	0.544
40	7.4	2.2	8.9	87.6	83.7	0.241	0.454	0.111	1.881	0.531
45	7.4	2.4	9.3	87.5	83.2	0.240	0.452	0.110	1.877	0.530
50	7.0	1.0	10.2	88.0	82.8	0.241	0.449	0.119	1.879	0.536
55	6.8	2.4	11.0	89.3	82.3	0.235	0.446	0.091	1.905	0.527
60	6.8	2.4	11.7	89.9	81.6	0.233	0.442	0.084	1.919	0.527
120	5.6	2.4	17.3	90.5	77.0	0.218	0.418	0.078	1.899	0.521
180	5.5	1.5	21.6	91.2	73.0	0.209	0.396	0.079	1.909	0.527
240	5.3	1.6	24.9	93.0	69.9	0.199	0.379	0.058	1.951	0.526
300	4.8	1.6	27.8	92.7	67.4	0.192	0.366	0.062	1.926	0.524
360	4.8	1.6	30.3	92.5	64.9	0.185	0.352	0.064	1.917	0.525
720	4.3	1.6	38.6	92.8	57.1	0.162	0.310	0.061	1.898	0.524
1440	4.0	1.6	48.4	92.7	47.6	0.136	0.258	0.062	1.863	0.526
2880	3.8	1.6	49.8	92.0	46.5	0.132	0.252	0.070	1.816	0.523
4320	3.6	1.8	49.8	93.2	46.6	0.131	0.253	0.053	1.864	0.519
5760	3.2	1.8	49.8	92.5	47.0	0.131	0.255	0.061	1.818	0.515

## **Monitoring of the self-assembly of the [Pd<sub>6</sub>L<sub>12</sub>](BF<sub>4</sub>)<sub>12</sub> complexes by ESI-TOF mass spectrometry**

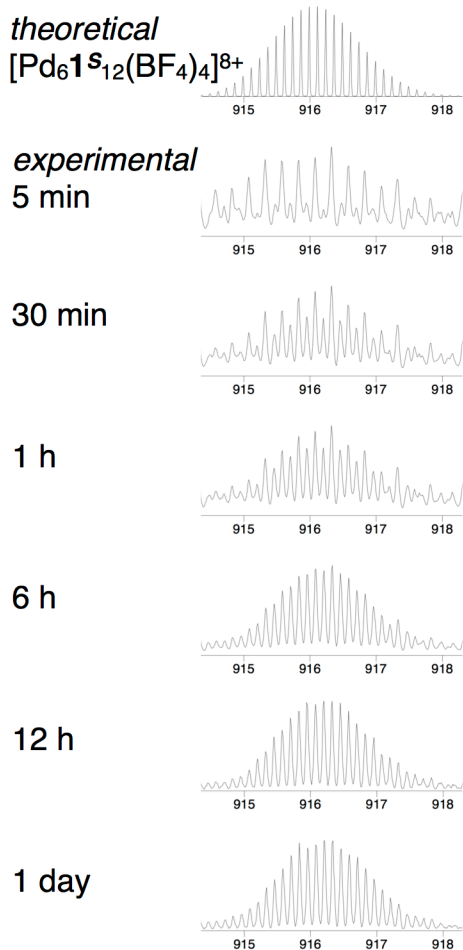
A solution of [PdPy\*<sub>4</sub>](BF<sub>4</sub>)<sub>2</sub> and L (**1<sup>S</sup>**, **2**, or **3**) were mixed in a 1:2 ratio in CD<sub>3</sub>NO<sub>2</sub> for **1<sup>S</sup>** ([**1<sup>S</sup>**]<sub>0</sub> = 1.8 mM) or a mixed solvent of CD<sub>3</sub>NO<sub>2</sub> and CD<sub>2</sub>Cl<sub>2</sub> (4/1, v/v) for **2** and **3** ([**2**]<sub>0</sub> = 1.9 mM and [**3**]<sub>0</sub> = 2.0 mM). At each time point, 50 μL of the reaction mixture was taken, diluted with CH<sub>3</sub>NO<sub>2</sub> (500 μL), filtered through a membrane filter (pore size: 0.20 μm) and injected in the mass spectrometer with 5.0 μL/min flow rate to obtain ESI-TOF mass spectra (Figures S4, S5, and S6 for [Pd<sub>6</sub>**1<sup>S</sup>**<sub>12</sub>](BF<sub>4</sub>)<sub>12</sub>, [Pd<sub>6</sub>**2**<sub>12</sub>](BF<sub>4</sub>)<sub>12</sub>, and [Pd<sub>6</sub>**3**<sub>12</sub>](BF<sub>4</sub>)<sub>12</sub>, respectively).



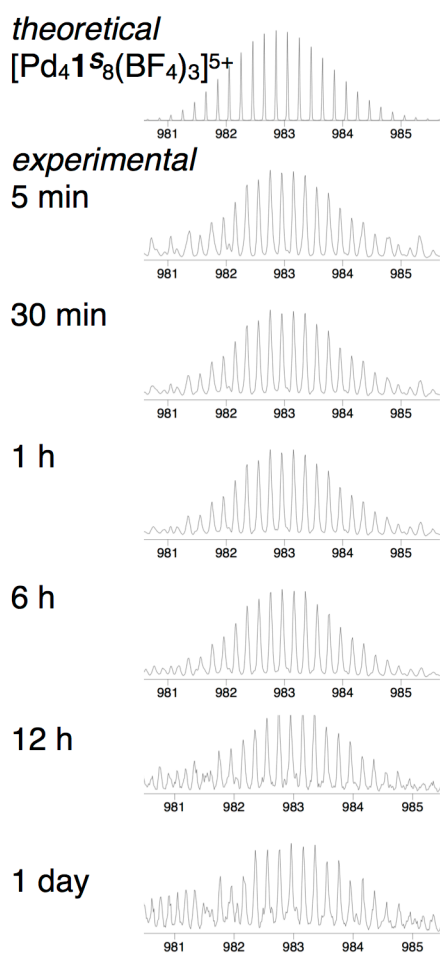




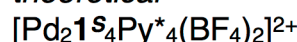
(l)



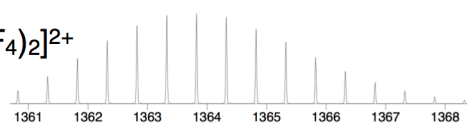
(m)



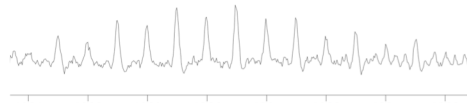
(n)

*theoretical**experimental*

5 min



30 min



1 h



6 h



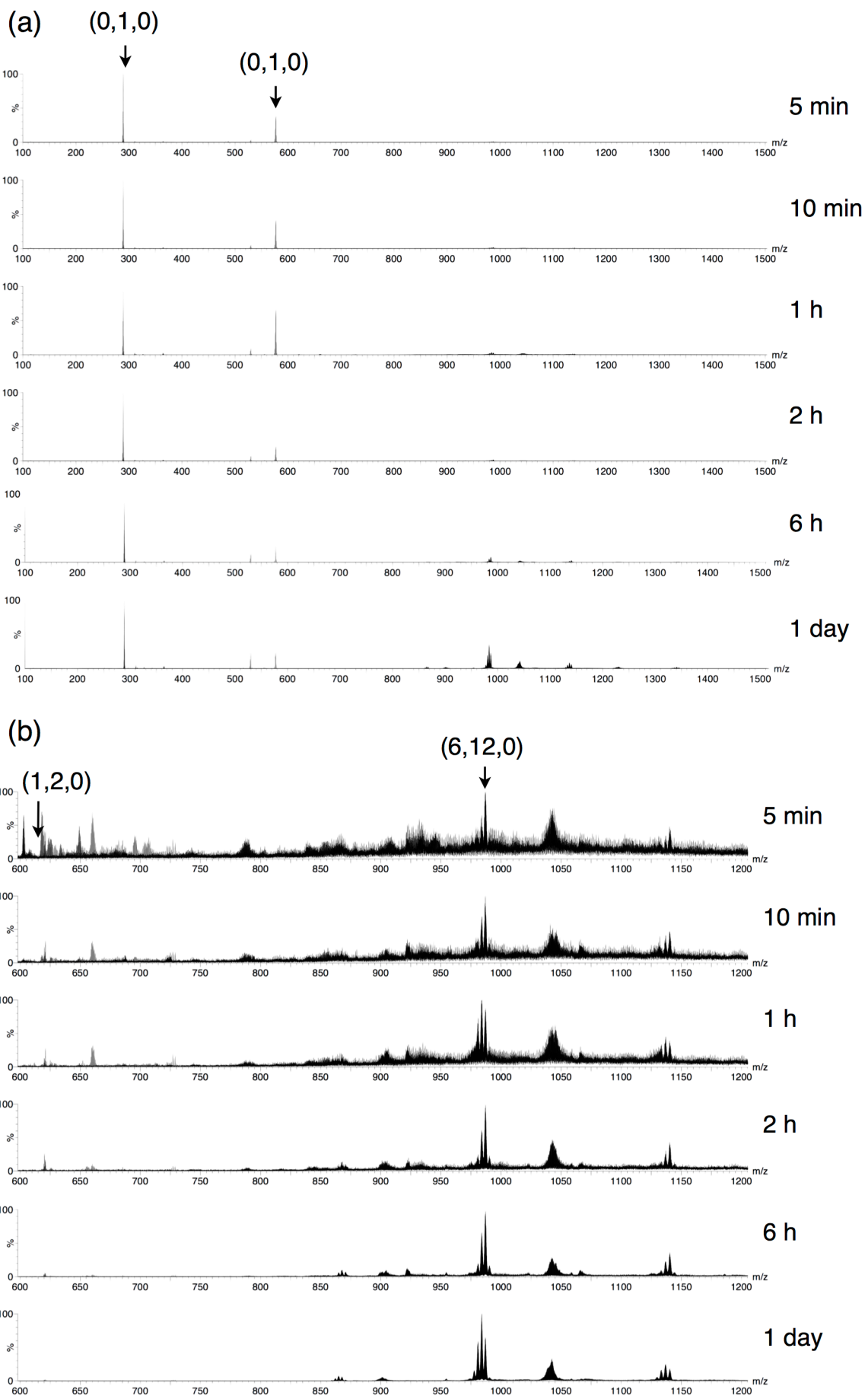
12 h

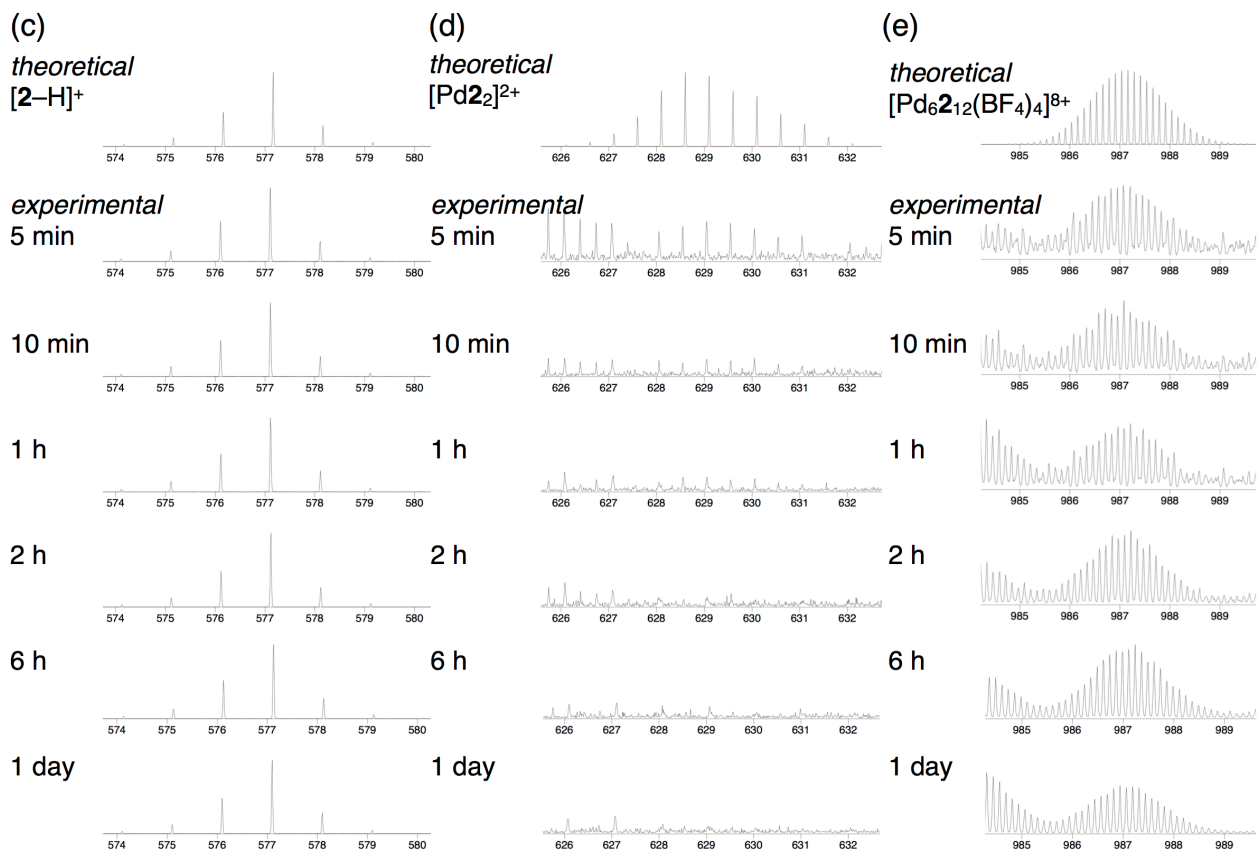


1 day

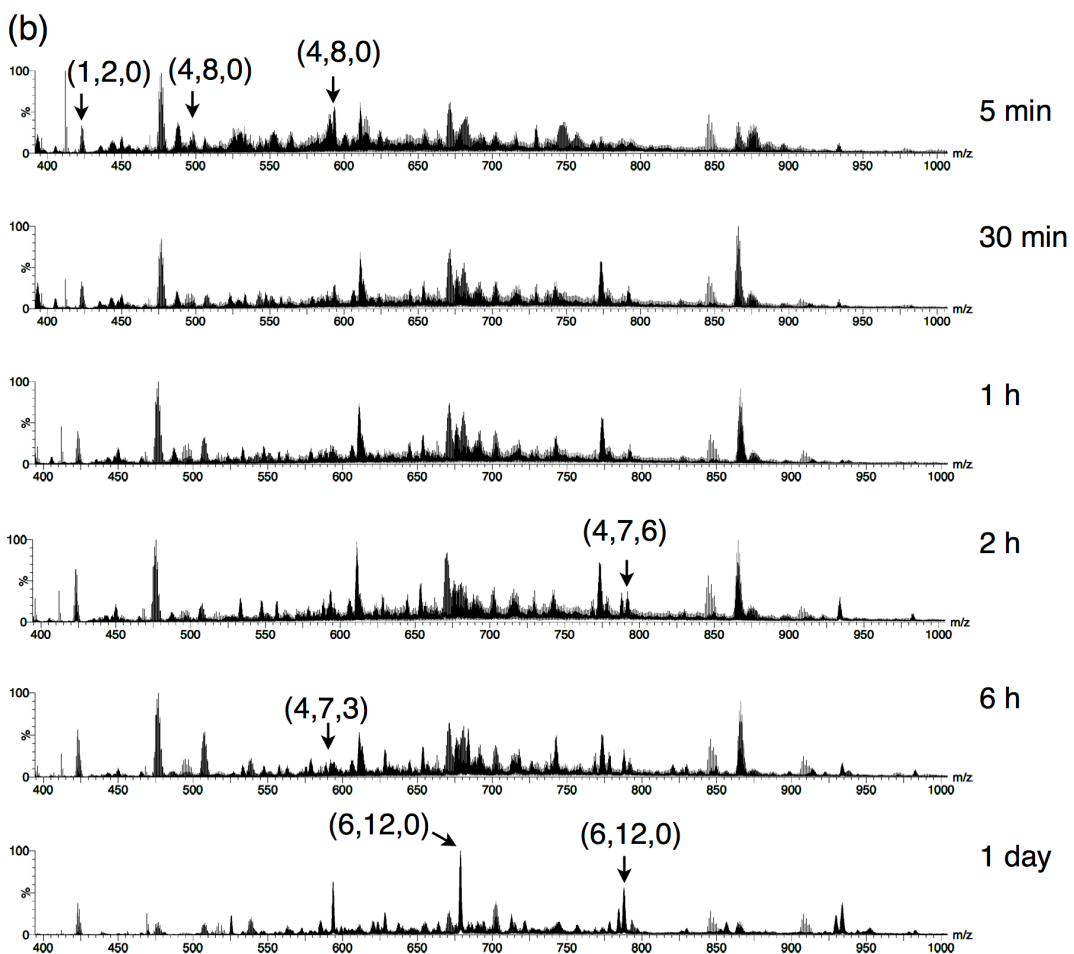
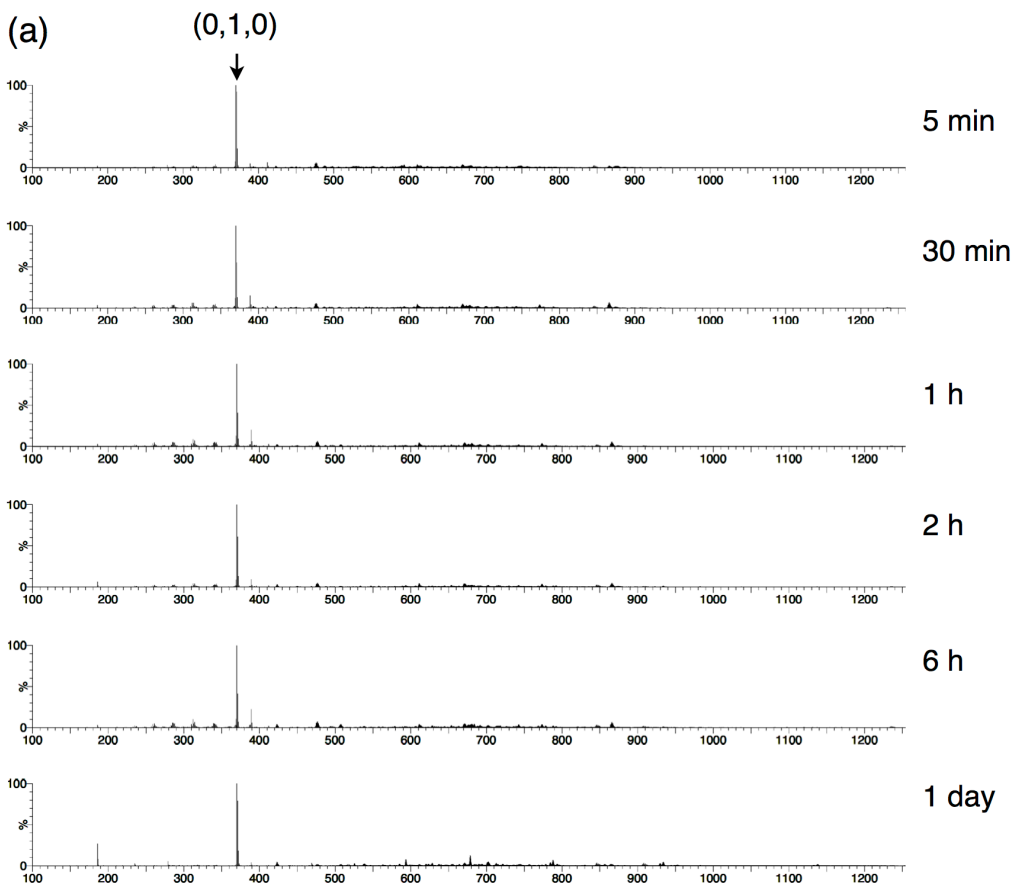


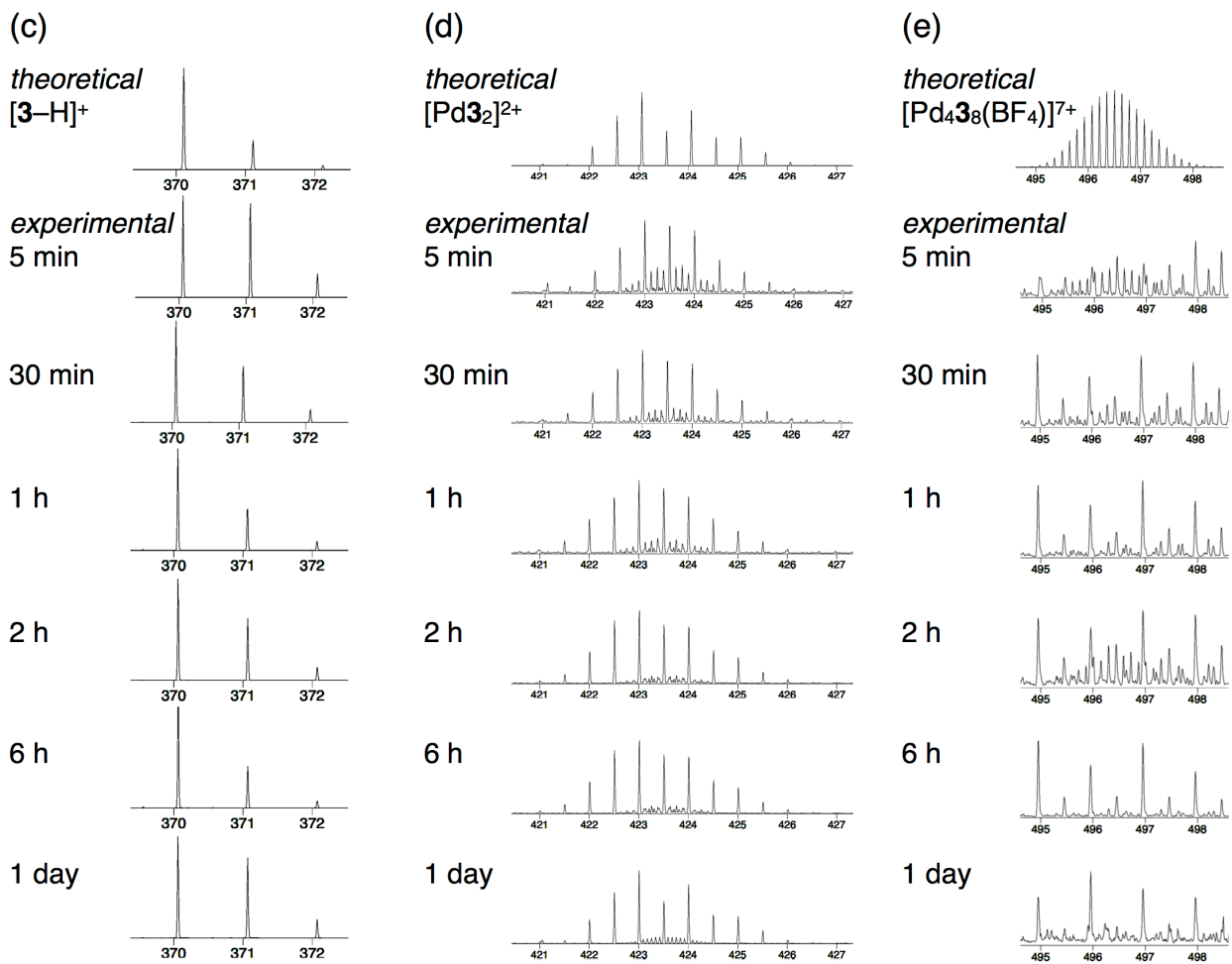
**Figure S4.** ESI-TOF mass spectra of the reaction mixture for the self-assembly of  $[\text{Pd}_6\mathbf{1}^S_{12}](\text{BF}_4)_{12}$  from **1**<sup>S</sup> and  $[\text{Pd}\text{Py}^*_4](\text{BF}_4)_2$  in  $\text{CD}_3\text{NO}_2$  at 298 K ( $[\mathbf{1}^S]_0 = 1.8 \text{ mM}$ ), measured at 5 min, 30 min, 1 h, 6 h, 12 h, and 1 day. Measurement condition: Capillary / 1.5 kV; Sampling Cone / 30 V; Source Offset / 80 V; Source / 80 °C; Desolvation / 150 °C; Cone Gas / 50 L h<sup>-1</sup>; Desolvation Gas / 800 L h<sup>-1</sup>. (a)  $m/z$ : 100–2500, (b)  $m/z$ : 550–2500, (c)  $[\text{Pd}_2\mathbf{1}^S_2\text{Py}^*_4]^{4+}$ , (d)  $[\text{Pd}_3\mathbf{1}^S_4\text{Py}^*_4]^{6+}$ , (e)  $[\text{Pd}_2\mathbf{1}^S_3\text{Py}^*_2]^{4+}$ , (f)  $[\mathbf{1}^S\text{-H}]^+$ , (g)  $[\text{Pd}_2\mathbf{1}^S_3\text{Py}^*_3]^{4+}$ , (h)  $[\text{Pd}_2\mathbf{1}^S_4\text{Py}^*_2]^{4+}$ , (i)  $[\text{Pd}_4\mathbf{1}^S_7\text{Py}^*_2(\text{BF}_4)_2]^{6+}$ , (j)  $[\text{Pd}_3\mathbf{1}^S_6\text{Py}^*_2(\text{BF}_4)]^{5+}$ , (k)  $[\text{Pd}_5\mathbf{1}^S_{10}(\text{BF}_4)_3]^{7+}$ , (l)  $[\text{Pd}_6\mathbf{1}^S_{12}(\text{BF}_4)_4]^{8+}$ , (m)  $[\text{Pd}_4\mathbf{1}^S_8(\text{BF}_4)_3]^{5+}$ , (n)  $[\text{Pd}_2\mathbf{1}^S_4\text{Py}^*(\text{BF}_4)_2]^{2+}$ . (a, b, c) indicates species  $[\text{Pd}_a\mathbf{1}^S_b\text{Py}^*_c]^{2a+}$ .





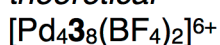
**Figure S5.** ESI-TOF mass spectra of the reaction mixture for the self-assembly of  $[Pd_6\mathbf{2}_{12}](BF_4)_{12}$  from **2** and  $[PdPy^*_4](BF_4)_2$  in  $CD_3NO_2$  and  $CD_2Cl_2$  (4:1, v/v) at 298 K ( $[2]_0 = 1.9$  mM), measured at 5 min, 10 min, 1 h, 2 h, 6 h, and 1 day. Measurement condition: Capillary / 1.5 kV; Sampling Cone / 30 V; Source Offset / 80 V; Source / 80 °C; Desolvation / 150 °C; Cone Gas / 50 L h<sup>-1</sup>; Desolvation Gas / 800 L h<sup>-1</sup>. (a)  $m/z$ : 100–1500, (b)  $m/z$ : 600–1200, (c)  $[2-H]^+$ , (d)  $[Pd_2]^{2+}$ , and (e)  $[Pd_6\mathbf{2}_{12}(BF_4)_4]^{8+}$ . (a, b, c) indicates species  $[Pd_a\mathbf{2}_bPy^*_c]^{2a+}$ .



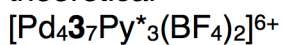


(f)

*theoretical*

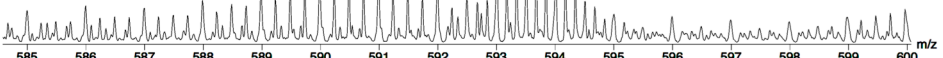


*theoretical*

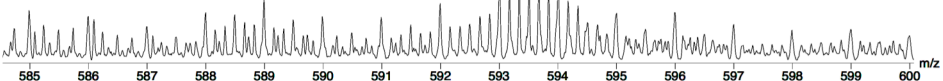


*experimental*

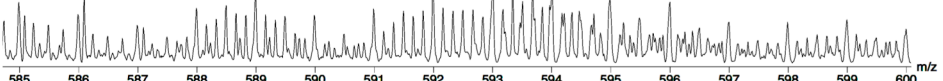
5 min



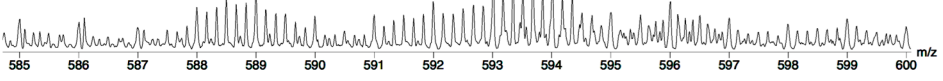
30 min



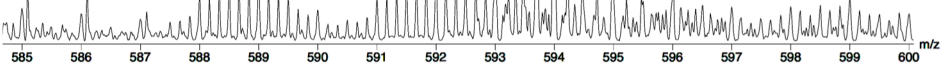
1 h



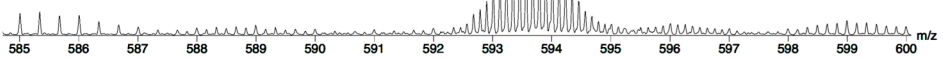
2 h



6 h



1 day



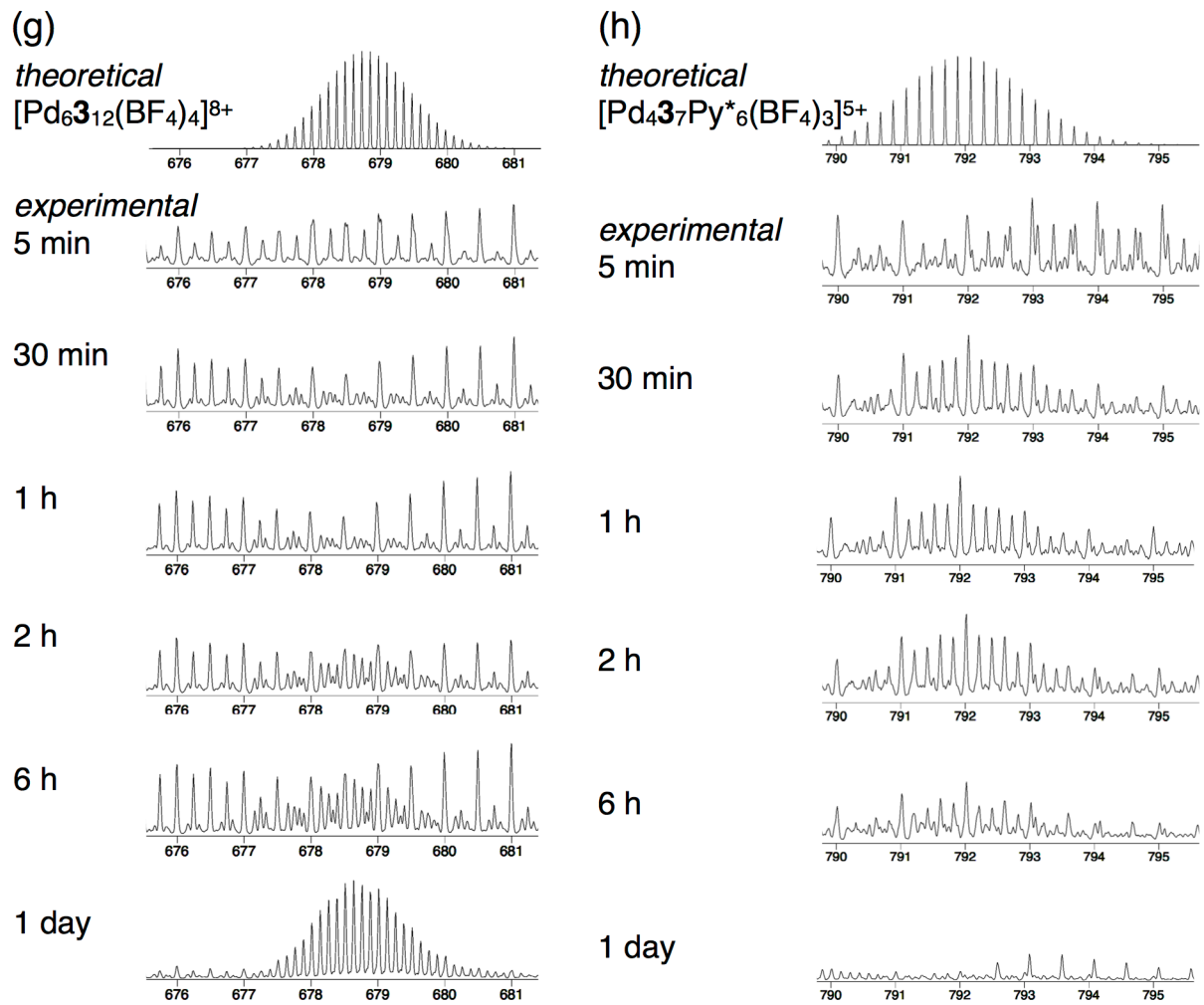


**Figure S6.** ESI-TOF mass spectra of the reaction mixture for the self-assembly of  $[\text{Pd}_6\mathbf{3}_{12}](\text{BF}_4)_{12}$  from **3** and  $[\text{Pd}\text{Py}^*_{\cdot 4}](\text{BF}_4)_2$  in  $\text{CD}_3\text{NO}_2$  and  $\text{CD}_2\text{Cl}_2$  (4:1, v/v) at 298 K ( $[\mathbf{3}]_0 = 2.0 \text{ mM}$ ), measured at 5 min, 30 min, 1 h, 2 h, 6 h, and 1 day. Measurement condition: Capillary / 3.0 kV; Sampling Cone / 30 V; Source Offset / 80 V; Source / 80 °C; Desolvation / 150 °C; Cone Gas / 50 L h<sup>-1</sup>; Desolvation Gas / 800 L h<sup>-1</sup>. (a)  $m/z$ : 100–1300, (b)  $m/z$ : 400–1000, (c)  $[\mathbf{3}-\text{H}]^+$ , (d)  $[\text{Pd}\mathbf{3}_2]^{2+}$ , (e)  $[\text{Pd}_4\mathbf{3}_8(\text{BF}_4)]^{7+}$ , (f)  $[\text{Pd}_4\mathbf{3}_8(\text{BF}_4)_2]^{6+}$  and  $[\text{Pd}_4\mathbf{3}_7\text{Py}^*\mathbf{3}(\text{BF}_4)_2]^{6+}$ , (g)  $[\text{Pd}_6\mathbf{3}_{12}(\text{BF}_4)_4]^{8+}$ , and (h)  $[\text{Pd}_4\mathbf{3}_7\text{Py}^*\mathbf{6}(\text{BF}_4)_3]^{5+}$ . (a, b, c) indicates species  $[\text{Pd}_a\mathbf{3}_b\text{Py}^*_{\cdot c}]^{2a+}$ .

## Molecular modeling study

Geometry optimization was performed by molecular mechanics (*MM*) calculation with Universal Force field (BIOVIA Material Studio 2017 R2, Accelrys Software Inc.).

**Optimized structures of double-walled motifs *cis*-[Pd<sub>2</sub>L<sub>2</sub>Py<sub>4</sub>]<sup>4+</sup> (Py: pyridine) for ditopic ligands **2** and **3****

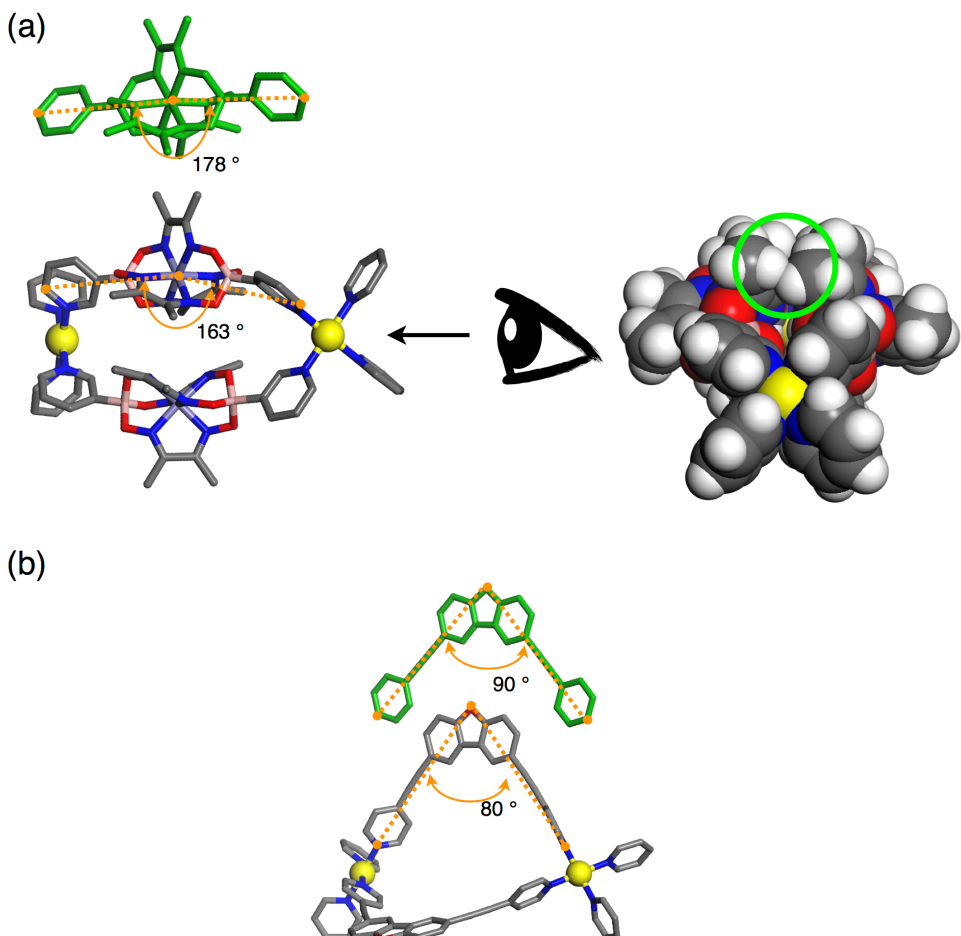


**Figure S7.** Optimized structures by *MM* calculation. Color labels: yellow, Pd; grey, C; blue, N; red, O; pink, B and purple, Fe. (a) *cis*-[Pd<sub>2</sub>**2**Py<sub>4</sub>]<sup>4+</sup>. A stick model in green indicates optimized structure of **2**. A CPK model shown in the right is a side view of a ball-and-stick model. A green circle indicates the steric repulsion between methyl groups. (b) *cis*-[Pd<sub>2</sub>**3**<sub>2</sub>Py<sub>4</sub>]<sup>4+</sup>. A stick model in green indicates optimized structure of **3**.

## References

- (1) Gütz, C.; Hovorka, R.; Klein, C.; Jiang, Q. Q.; Bannwarth, C.; Engeser, M.; Schmuck, C.; Assenmacher, W.; Mader, W.; Topić, F.; Rissanen, K.; Grimme, S.; Lützen, A. *Angew. Chem. Int. Ed.* **2014**, *53*, 1693–1698.
- (2) Wise, M. D.; Holstein, J. J.; Pattison, P.; Besnard, C.; Solari, E.; Scopelliti, R.; Bricogne, G.; Severin, K. *Chem. Sci.* **2015**, *6*, 1004–1010.
- (3) Suzuki, K.; Tominaga, M.; Kawano, M.; Fujita, M. *Chem. Commun.* **2009**, 1638–1640.
- (4) Tateishi, T.; Zhu, W.; Foianesi-Takeshige, L. H.; Kojima, T.; Ogata, K.; Hiraoka, S. *Eur. J. Inorg. Chem.* **2018**, 1192–1197.